

# COSMIC ACCELERATION FROM CAUSAL BACKREACTION WITH RECURSIVE NONLINEARITIES

Brett Bochner

*Department of Physics and Astronomy, Hofstra University, Hempstead, NY 11549*

brett.bochner@alum.mit.edu, phybdb@hofstra.edu

## ABSTRACT

We revisit the causal backreaction paradigm, in which the need for Dark Energy is eliminated via the generation of an apparent cosmic acceleration from the causal flow of inhomogeneity information coming in towards each observer from distant structure-forming regions. A second-generation version of this formalism is developed, now incorporating the effects of “recursive nonlinearities”: the process by which metric perturbations already established by some given time will subsequently act to slow down all future flows of inhomogeneity information. In this new formulation, the long-range effects of causal backreaction are damped, substantially weakening its impact for simulated models that were previously best-fit cosmologies. Despite this result, we find that causal backreaction can be recovered as a replacement for Dark Energy through the adoption of larger values for the dimensionless ‘strength’ of the clustering evolution functions being modeled – a change justified by the hierarchical nature of clustering and virialization in the universe, occurring as it does on multiple cosmic length scales simultaneously. With this and with the addition of one extra model parameter used to represent the slowdown of clustering due to astrophysical feedback processes, an alternative cosmic concordance can once again be achieved for a matter-only universe in which the apparent acceleration is generated entirely by causal backreaction effects. The only significant drawback is a new degeneracy which broadens our predicted range for the observed jerk parameter  $j_0^{\text{Obs}}$ , thus removing what had appeared to be a clear signature for distinguishing causal backreaction from Cosmological Constant  $\Lambda$ CDM. Considering the long-term fate of the universe, we find that incorporating recursive nonlinearities appears to make the possibility of an ‘eternal’ acceleration due to causal backreaction far less likely; though this conclusion does not take into account potential influences due to gravitational nonlinearities or the large-scale breakdown of cosmological isotropy, effects not easily modeled within this formalism.

*Subject headings:* cosmological parameters — cosmology: theory — dark energy  
— large-scale structure of universe

## 1. INTRODUCTION: COSMIC CONCORDANCE AND CAUSAL BACKREACTION

One of the key questions in Cosmology today relates to the still-unsolved problem of what is causing the observed cosmic acceleration. Primarily indicated by Hubble curves constructed from luminosity distance measurements of Type Ia supernovae (Perlmutter et al. 1999; Riess et al. 1998), this (possibly apparent) acceleration is just one aspect of the struggle for a consistent picture of the universe; a picture that would also require an explanation of the gap between the observed clustering matter content of  $\Omega_M \sim 0.3$  (e.g., Turner 2002a) and the value of  $\Omega_{\text{Tot}} = 1$  as indicated by Cosmic Microwave Background measurements of spatial flatness (Komatsu et al. 2011), as well as a solution of the “Age Problem/Crisis” for matter-only (i.e., decelerating) cosmologies in which the universe appears to be younger than some of its oldest constituents (e.g., Turner 2002b), along with explanations of other important issues.

The standard approach to solving these problems is to introduce some form of “Dark Energy” – the simplest case being the Cosmological Constant,  $\Lambda$  – which can fill the gap via  $\Omega_{\text{DE}} = \Omega_{\text{Tot}} - \Omega_M \sim 0.7$ , which possesses negative pressure in order to achieve cosmic acceleration (e.g., Kolb & Turner 1990), and which (for non- $\Lambda$  cases) recruits some form of internal nonadiabatic pressure (e.g., Caldwell et al. 1998) in order to avoid clustering as matter does. Thus the introduction of Dark Energy (often using spatially-flat  $\Lambda$ CDM models) has led to a broadly-consistent “Cosmic Concordance” – an empirical outline which has seemed so far to succeed fairly well (e.g., Komatsu et al. 2011) at developing into a consistent cosmological picture.

There are serious aesthetic problems with Dark Energy, however, as is well known; the most obvious being the problematical introduction of a completely unknown substance as the dominant component of the universe. Beyond that, a static (i.e., Cosmological Constant) form of Dark Energy suffers from two different fine-tuning problems: one being the issue that  $\rho_\Lambda$  is  $\sim 120$  orders of magnitude smaller than what would be expected from the Planck scale (Kolb & Turner 1990); and the other being a “Coincidence Problem” (e.g., Arkani-Hamed et al. 2000), questioning why observers *today* happen to live so near the onset of  $\Lambda$ -domination, given  $\rho_\Lambda/\rho_M \propto a^3$ . Moving to a dynamically-evolving Dark Energy

(DDE), however, invites other problems, since the *self-attractive* nature of negative-pressure substances (i.e.,  $\partial E/\partial V = -P > 0$ ) means that a DDE may cluster spatially (Caldwell et al. 1998), possibly ruining it as a “smoothly-distributed” cosmic ingredient. This could potentially be solved through the ad-hoc addition of some form of nonadiabatic support pressure for the DDE (Hu 1998), but this is a possibility which we have argued against elsewhere (Bochner 2011) on thermodynamically-based cosmological grounds.

Besides Dark Energy, various other methods have been used to attempt to explain the observed acceleration, such as employing modified gravity (e.g., Trodden 2008), or assuming the existence of an underdense void centered not too far from our cosmic location (e.g., Tomita 2001). But to avoid the substantial (and perhaps needless) complications which arise when assuming departures from General Relativity, as well as the non-Copernican ‘specialness’ implied by a local void, we will instead use the feedback from cosmological structure formation itself as a *natural* trigger for the onset of acceleration – a trigger that automatically activates at just the right time for observers to see it, due to the fact that all such observers will have been created by that very same structure formation which generates the observed cosmic acceleration.

This approach, known generally as “backreaction”, was used by this author in Bochner (2011) (henceforth BBI) to find several clustering models which managed to precisely reproduce the apparent acceleration seen in Hubble curves of Type Ia supernova standard candles, while simultaneously driving a number of important cosmological parameters to within a close proximity of their Concordance values – including the age of the universe, the matter density required for spatial flatness, the present-day deceleration parameter, and the angular scale of the Cosmic Microwave Background.

The ability of our models to achieve these goals, despite the generally pessimistic view of backreaction typically held by researchers currently (e.g., Schwarz 2010), was due to our adoption of an explicitly causal variety of backreaction, which admits the possibility of substantial backreaction from Newtonian-strength perturbations. The standard formalism used for computing backreaction effects, developed through the extensive work of Buchert and collaborators (e.g., Buchert & Ehlers 1997; Buchert et al. 2000), is non-causal in the sense that it drops all ‘gravitomagnetic’ (i.e., velocity-dependent) effects, thus rendering it unable to account for metric perturbation information flowing (at the speed of null rays) from structures forming in one part of the universe, to observers in another. In similar fashion, typical studies of cosmic structure formation are also non-causal in that they use the Poisson equation without time derivatives of the perturbation potential, thus computing metric perturbations from *local* matter inhomogeneities only, disregarding all gravitational information coming in from elsewhere in space. The result is a mistaken (but widespread)

notion that the entire Newtonian backreaction  $Q_N$  can be expressed mathematically as a total divergence, thus ultimately rendering it negligible. But by restoring causality with a “causal updating” integral that incorporates perturbations to an observer’s metric coming from inhomogeneities all the way out to the edge of their observational horizon, we find (BBI) that the sum of such ‘innumerable’ Newtonian-strength perturbations – which increase in number as  $r^2$  within a spherical shell at distance  $r$  from the observer, more than compensating for their  $1/r$  weakening with distance – adds up to a total backreaction effect that is not only non-negligible (regardless of the smallness of  $v^2/c^2$  for most matter flows), but is in fact a dominant cosmological effect that is fully capable of reproducing the observed cosmic acceleration in a fully ‘concordant’ manner.

Despite these successes, a major problem with our model in BBI is its utter simplicity: it is clearly a toy model, with the results presented there serving primarily as ‘proof-of-principle’ tests, rather than as precision cosmological predictions. Though the simplifications of the model are many, one in particular is serious in its consequences, while fortunately being not too difficult to fix: specifically, this is the dropping of what we have termed “recursive nonlinearities”. Unrelated to *gravitational* nonlinearities, or to the nonlinear regime of density perturbations in structure formation, recursive nonlinearities embody the fact that the integrated propagation time of a null ray carrying perturbation information to an observer from a distant virializing structure would itself be affected by all of the other perturbation information that has already come in to cross that ray’s path from everywhere else, during all times prior to arrival. In other words, causal updating is itself slowed by the metric perturbation information carried by causal updating, creating an operationally nonlinear problem.

This issue was necessarily neglected in BBI, as that work was devoted to introducing our ‘zeroth-order’ approach to causal backreaction. But here we fix this problem, incorporating recursive nonlinearities into a new, ‘first-order’ version of our phenomenological model. We will find that this alteration significantly changes our results, causing a profound weakening of the backreaction effects generated by a given level of clustering, as well as significantly damping the long-term effects of information from old perturbations coming in from extreme distances. In order to retain causal backreaction as a viable model for generating the observed cosmic acceleration – presuming here that this should indeed be done – it will be necessary to re-interpret the meaning of our (inherently empirical) ‘clumping evolution functions’ to now consider the effects of hierarchical clustering on a variety of cosmic scales. Doing this, we will show that a successful alternative concordance can once again be achieved, with the right amount (and temporal behavior) of acceleration, and with good cosmological parameters.

This paper will be organized as follows: in Section 2, we will re-introduce our original

causal backreaction formalism, and then describe the changes implemented in order to incorporate recursive nonlinearities into the model. In Section 3, we will explore the results of the new formalism, and discuss the implications of the model parameters that are now needed to achieve good data fits. Furthermore, we will discuss how the damping effects due to recursive nonlinearities would alter the key factors that determine the ‘ultimate’ fate of the universe, as was discussed for our original formalism in BBI, given an acceleration driven by causal backreaction rather than by some form of Dark Energy. Finally, in Section 4, we conclude with a summary of these ideas and results, highlighting the role of causal backreaction as a fundamental component of cosmological analysis and modeling.

## 2. THE CAUSAL BACKREACTION FORMALISM: OLD METHODS AND NEW DEVELOPMENTS

### 2.1. The Original Toy Model, and its Approximations and Simplifications

We recall here that the basic premise of the formalism developed in BBI is to phenomenologically represent the physical processes of structure formation – complex even at the level of Newtonian-strength gravitational perturbations – in a simple and convenient way. The physics at work within most clustering masses should be as follows: collapsing overdensities stabilize themselves and halt their collapse by concentrating their local vorticity (or equivalently, by creating a large local velocity dispersion); this concentrated vorticity or velocity dispersion leads to real, extra volume expansion in accordance with the Raychaudhuri equation (Hawking & Ellis 1973), representable (in the final state) at great distances by the tail of a Newtonian potential perturbation to the background Friedman Robertson-Walker (FRW) metric; and this Newtonian tail propagates causally outward into space by inducing inward mass flows towards the virialized object from farther and farther distances as time passes. The total perturbation at time  $t$  for any location in space – which will be independent of position, assuming similar structure formation rates everywhere – will then be the combined effects of innumerable Newtonian tails of this type, coming in towards the observer from the virializing masses (in all directions) which by that observation time have entered within the observer’s cosmological “clustering horizon”.

As is well known, the expansion evolution (i.e., the Friedmann equation) for some spherical volume  $\mathbf{V}$  can be derived – using nonrelativistic Newtonian equations, in fact, for a matter-dominated universe (Weinberg 1972, pp. 474-475) – without reference to anything outside of that sphere. In contrast, the Newtonian-level backreaction terms which we utilize here are due to perturbation information coming in from structures located predominantly outside of  $\mathbf{V}$  (since one must go to cosmological distances for the effects to add up signifi-

cantly). For any condensed structure (at great distance) which provides a gravitational pull upon the mass in  $\mathbf{V}$ , its main perturbative effect is simply to impose an extra (Newtonian) perturbation potential upon  $\mathbf{V}$  as an addition to its original cosmological metric. Our phenomenological approach, therefore, is one in which we model the inhomogeneity-perturbed evolution of  $\mathbf{V}$  with a metric that contains the individually-Newtonian contributions to the perturbation potential within  $\mathbf{V}$  (“ $\Phi_{\mathbf{V}}(t)$ ”) from all clumped, virialized structures outside of  $\mathbf{V}$  that have been causally ‘seen’ within  $\mathbf{V}$  by time  $t$ , superposed *on top of* the background Friedmann expansion of  $\mathbf{V}$ .

We will reiterate the mathematical essentials of this formalism below, in Section 2.2; but first we must recount the various approximations and simplifications which have gone into our analysis, to consider their importance and the feasibility of eliminating them in order to develop a greater degree of physical realism in these causal backreaction models.

First of all, though our backreaction-induced metric perturbations will indeed be time-dependent (due to the causal flow of inhomogeneity information), they will be entirely spatially-*independent*. As noted above, we do not seek to achieve an observed acceleration through the mechanism of a local void; but going even further, our model does not explicitly include any spatial variations whatsoever. Rather, the system being modeled is what we term a “smoothly-inhomogeneous” universe, in which all perturbation information blends together evenly in a way that is essentially independent of cosmic position.

Now, this simplification is one made out of practical necessity, not physical realism. The smoothly-inhomogeneous approximation relies upon an assumption of randomly-distributed clustering – which is certainly not true, as large clusters are not independent of each other, but preferentially clump near one another and are mutually correlated – and this becomes ever less true during the ongoing cosmic evolution, as the universe grows more inhomogeneous with time. Furthermore, this simplification relies upon the assumption that the region of space responsible for the dominant contributions to causal backreaction within volume  $\mathbf{V}$  will be large enough to contain a cosmologically-representative sample of both clusters and voids; but as we will see below in Section 3, adding in recursive nonlinearities (to correct another simplification, as described below) greatly reduces the size of the cosmological region affecting  $\mathbf{V}$  from what it was in our original toy model, potentially calling this assumption into question.

A proper accounting of causal backreaction in a realistically inhomogeneous universe would require the implementation of a fully spatially-detailed, three-dimensional cosmic structure simulation program – perhaps along the lines of Springel et al. (2005), for example – but with Newtonian-level backreaction effects from causal updating now added in. The development of such a 3D simulation model is far beyond the scope of this paper (and beyond

the efforts of any individual researcher), but would be a useful mission to be undertaken by the cosmological community at large.

A second simplification is our use of Newtonian potential terms – i.e., the long-distance approximation of the Schwarzschild metric (e.g., Weinberg 1972) – to represent the tail of each individual perturbation felt from far away, rather than using a long-distance approximation of the Kerr metric for spinning masses (Kerr 1963), despite the crucial role of some form of vorticity in stabilizing most structures against singular collapse. In this case, however, the approximation is a good one. A relatively small amount of vorticity can suffice for the self-stabilization of a clumped mass, if it is applied perpetually; and the specific angular momentum (i.e.,  $[J/(Mc)]$ ) will be small for any mass not on the verge of being an extremal black hole. Furthermore, it is easy to show (e.g., Franklin & Baker 2007) that the highest-order deviations from the Newtonian expression in the diagonal metric components will go like  $[J/(Mc)]^2$ , thus being entirely negligible at the huge distances relevant for causal backreaction. (And the leading-order *off-diagonal* Kerr perturbation terms, though actually proportional to  $(J/r)$ , will effectively cancel out due to angle-averaging in the smoothly-inhomogeneous approximation, as discussed in BBI.) Thus it appears quite safe to ignore any Kerr-specific perturbation effects for physically reasonable situations.

Third, our formalism neglects the purely observational effects of localized inhomogeneities, such as lensing along beam paths (e.g., Kantowski 2003) for rays from standard candles, and similar perturbative effects upon the apparent luminosity distance relationship for rays passing through inhomogeneous regions, which in some models represents the primary ‘backreaction’ effect resulting from structure formation (e.g., Biswas et al. 2007). Even if such effects by themselves are too small to generate an observed cosmic acceleration, they will still alter the output parameters estimated while using any cosmological model (including ours), and thus should be kept track of; and in case our causal backreaction method also falls short of providing the full result of an apparent acceleration all by itself, it might successfully be combined with these other observational effects upon the light rays to produce an apparent acceleration once everything is added together (this point to be discussed again in Section 3.1). Combining these purely observational effects with those from causal backreaction is therefore an important task, and likely quite a feasible one; though not one addressed yet in this current paper.

The next, most theoretically treacherous approximation is our neglect of nonlinear gravitational effects, a simplification made implicitly by our method of linearly adding together the individual metric perturbations contributed by different self-stabilized mass ‘clumps’ in order to produce the total, summed, Newtonian-strength perturbation potential. (Note that this is not the full “Newtonian” approximation usually employed, since while we do

assume weak-gravity, we do not completely assume ‘slow-motion’ – in the sense of dropping all time derivatives of the perturbation potential – as that would neglect the causal flow of perturbation information.) Thus our formalism explicitly neglects the nonlinear, purely general-relativistic effects that most other researchers primarily focus upon when studying “backreaction”. This approximation becomes increasingly bad as the magnitude of the summed perturbation potential approaches unity; but since (as will be seen below) this potential typically does not grow to values in excess of  $\sim 0.5 - 0.6$  or so as  $t \rightarrow t_0$  for most of our best-fitting simulation runs, the approximation is probably good enough for our simulations to provide fairly accurate estimations of the cosmic evolution up to now, and of our measurable cosmological parameters. (And to the extent that it is not good enough, a significant contribution due to nonlinear gravitational terms would likely only help produce the desired acceleration even more easily.) Thus it is probably not necessary for us to include higher-order gravitational terms in our formalism, in order to achieve a sufficiently reliable understanding of the currently-observable universe for our present purpose of pointing the way towards an alternative concordance; a fortunate situation, since our model is fundamentally designed around a linearized-gravity approach, and it may be challenging to find any convenient way of modifying it to include nonlinear gravitational effects. On the other hand, given the ever-increasing strength of gravitational nonlinearities in the cosmos over time, a fully general-relativistic model of causal backreaction (computed using a 3D simulation of realistically-distributed inhomogeneities) would almost certainly be necessary for accurately predicting the long-term future evolution of the universe.

Lastly, there is the approximation regarding what we have referred to as “recursive nonlinearities”. As will be seen from the metric given below in Section 2.2, one of the effects of causal backreaction is real extra volume creation. But since causal backreaction depends upon the propagation of inhomogeneity information through space, the extra volume produced by old information from perturbations will slow down the propagation of all future inhomogeneity information (as well as carrying all perturbing masses farther away from all observation points), thus feeding back upon the causal backreaction process in such a way as to strongly dampen it. Of all of the simplifications and approximations discussed so far in this subsection, the neglect of these recursive nonlinearities most likely has the strongest impact upon the quantitative predictions emerging from our causal backreaction models. Fortunately, however, fixing this problem by adding these recursive nonlinearities into our formalism is one of the simpler improvements in physical realism for us to make; and hence, this paper focuses upon achieving this fix, and then calculating and interpreting the results produced by this ‘second-generation’ causal backreaction formalism.



## 2.2. The Old Formalism and its Results

Here we recall the technical details of our original formalism developed in BBI, to set the stage for its further development to follow.

To obtain the Newtonian approximation of a single ‘clumped’ (i.e., virialized, self-stabilized) object of mass  $M$ , embedded at the origin ( $r = 0$ ) in an expanding, spatially-flat, matter-dominated (MD) universe, one may linearize the McVittie solution (McVittie 1933), as can be seen from the perturbed FRW expression given in Kaloper et al. (2010). The resulting Newtonian-perturbed FRW cosmology is given by the metric:

$$ds^2 \approx -c^2[1 + (2/c^2)\Phi(t)]dt^2 + [a_{\text{MD}}(t)]^2[1 - (2/c^2)\Phi(t)]dr^2 + [a_{\text{MD}}(t)]^2r^2[d\theta^2 + \sin^2\theta d\phi^2], \quad (1)$$

where  $\Phi(t) \equiv \{-GM/[a_{\text{MD}}(t)r]\}$ , and  $a_{\text{MD}}(t) \propto t^{2/3}$  is the unperturbed MD scale factor evolution function.

For our model of a smoothly-inhomogeneous universe, we assume a random distribution of clustered masses, being the same essentially everywhere and in every direction. So turning the above expression around, we consider the situation for an observer at the origin, whose metric is affected by a collection of (roughly identical) discrete masses – for now confined to a spherical shell at coordinate distance  $r'$ , and with *total* mass  $M$  – that are distributed randomly in direction. The different directions of the various clumps does not matter for the observer’s  $g_{tt}$  metric component; but it does matter for the spatial metric components, due to the fact that a spatial displacement from the origin would pick up (direction-dependent) factors of  $\cos^2\theta$  in  $ds^2$  from the different angles of the motion with respect to the individual clumped masses, since only the radial projection of a given translation (with respect to a particular clump) will ‘feel’ the perturbation potential from that clump in its contribution (all within  $g_{rr}$ ) to the interval  $ds^2$ . Averaging over direction in three dimensions, the spatial metric terms therefore pick up a factor of  $\langle \cos^2\theta \rangle = (1/3)$  for the total effect when summing over all of the discrete masses; and the total, (gravitationally-)linearly summed and angle-averaged metric for this observer at the origin can then be written in ‘isotropized’ fashion, as:

$$ds^2 = -c^2\{1 - [R_{\text{Sch}}(t)/r']\} dt^2 + [a_{\text{MD}}(t)]^2\{1 + (1/3)[R_{\text{Sch}}(t)/r']\} |d\vec{r}|^2, \quad (2)$$

where  $R_{\text{Sch}}(t) \equiv \{(2GM/c^2)/[a_{\text{MD}}(t)]\}$ , and  $|d\vec{r}|^2 \equiv (dr^2 + r^2d\theta^2 + r^2\sin^2\theta d\phi^2) = |d\vec{x}|^2 \equiv (dx^2 + dy^2 + dz^2)$ . (Note that this factor of 1/3 is not ‘fundamental’, but is merely the result of our approximating the linearized sum of many individual ‘Newtonian’ solutions, which effectively spreads out the total spatial perturbation among all three spatial metric terms, rather than confining it solely to  $g_{rr}$ , as is usual. Thus the general relativistic expectation of equal temporal and spatial potentials – i.e.,  $\psi = \phi$  – is not really violated here, and no actual new physics or modified gravity is implied by it.) We regard the term multiplying

$[a_{\text{MD}}(t)]^2 |d\vec{r}|^2$  as a ‘true’ increase in spatial volume, and the  $g_{tt}$  term as an ‘observational’ term, slowing down the perceptions of observers at any given  $t$ . Thus, even if the spatial term by itself is not sufficient to generate a real volumetric acceleration, the spatial and temporal perturbations coupled together may indeed be enough to create an “apparent acceleration” capable of explaining all relevant cosmological observations.

The expression in Equation 2 represents the perturbations to the metric due to masses at some specific coordinate distance  $r'$  – and thus from a specific look-back time  $t'$  – as seen from some particular observational point. The total metric at that spacetime point must be computed via an integration over all possible distances, out to the distance (and thus look-back time) at which the universe had been essentially unclustered. Finally, a light ray reaching us from its source (e.g., a Type Ia supernova being used as a standard candle) travels to us in a path composed of a collection of such points, where the metric at each point must be calculated via its own integration out to its individual “inhomogeneity horizon”; and only by calculating the metric at every point in the pathway from the supernova to our final location here at  $r = z = 0$  can we figure out the total distance that the light ray has been able to travel through the increasingly perturbed metric, given its emission at some specific redshift  $z$ .

Finite look-back times imply that when one is feeling the effects of clumps at cosmological distances, what one is really sampling is the clustering as it was at an earlier, retarded time. Thus the cosmological evolution at all times is dependent upon the entire history of the development of clustering. In BBI, we defined a heuristic “clumping evolution function”,  $\Psi(t)$ , intended to simply represent the fraction of the cosmic matter that has completed its relaxation to a self-stabilized, steady state by cosmic time  $t$ , as opposed to that mass still freely expanding (or collapsing) within a still dynamically-evolving patch of space. The function  $\Psi(t)$  was therefore defined over the range from  $\Psi(t) = 0$  (perfectly smooth matter), to  $\Psi(t) = 1$  (everything clumped). This is an extremely simplified way of representing the virialization of cosmic structures, and we will in fact be forced to re-evaluate the meaning (and the range) of the function  $\Psi(t)$  later on in this paper. But for now, we just recall that the specific functions used for  $\Psi(t)$  in our numerical simulations are not rigorously derived from first principles, but rather are adopted for simplicity, with their functional forms and input parameters being motivated by physically reasonable structure formation behaviors, in conjunction with certain quantitative cosmological measurements.

Now, to determine how Hubble curves obtained from standard candle measurements are calculated in our formalism, consider a light ray emitted by a supernova at cosmic coordinate time  $t = t_{\text{SN}}$ , which then propagates from the supernova at  $r = r_{\text{SN}}$ , to us at  $r = 0$ ,  $t = t_0$ . We refer here to the geometry depicted in Figure 1.

For each point  $P \equiv (r, t)$  of the trajectory, the metric at that point will be perturbed away from the background FRW form by all of the virialized clumps that have entered its causal horizon. Consider a sphere of (coordinate) radius  $\alpha$ , centered around point  $P$ , with coordinates  $(\alpha, t_{\text{ret}})$  (where  $t_{\text{ret}} \leq t$  is the retarded time), defined such that the information about the state of the clumping of matter on that sphere at time  $t_{\text{ret}}$  will arrive – via causal updating, traveling at the speed of null rays – to point  $P$  at the precise time  $t$ . To compute the fully-perturbed metric at  $P$ , we must integrate over the clumping effects of all such radii  $\alpha$ , from  $\alpha = 0$  out to  $\alpha_{\text{max}}$ , the farthest distance from  $P$  out from which clumping information can have causally arrived since the clustering of matter had originally begun in cosmic history.

For the remaining calculations in this subsection, note that we will be using our old formulation from BBI, *without* recursive nonlinearities (those changes will be presented later, in Subsection 2.3). In particular, this affects the speed of the propagation of inhomogeneity information through coordinate space (as well as some other issues), which for now will be calculated with respect to the *unperturbed* FRW backreaction metric, rather than referencing the perturbed metric itself in an explicitly self-consistent manner.

For an FRW metric with  $a(t) = a_0(t/t_0)^{2/3}$ , the coordinate distance traveled by a null ray in the cosmic time span from  $t_1$  to  $t_2$  will be  $\alpha \equiv (c/a_0) \int_{t_1}^{t_2} (t/t_0)^{-2/3} dt = [(3c/a_0)(t_0)^{2/3}(t_2^{1/3} - t_1^{1/3})]$ . Defining  $a_0 \equiv 3ct_0 = 2c/H_0$ , and with  $t_2 \equiv t$ ,  $t_1 \equiv t_{\text{ret}}$ , we thus have:  $\alpha = [(t/t_0)^{1/3} - (t_{\text{ret}}/t_0)^{1/3}]$ . We then turn this into a prescription for computing  $t_{\text{ret}}$  as a function of  $t$  (relative to the present time,  $t_0$ ) and  $\alpha$ , as follows:

$$t_{\text{ret}}(t, \alpha) = t_0[(t/t_0)^{1/3} - \alpha]^3 . \quad (3)$$

Similarly, we can determine  $\alpha_{\text{max}}$ , given some initial time  $t_{\text{Init}}$  at which structure formation can be reasonably said to have started (i.e.,  $\Psi(t \leq t_{\text{Init}}) \equiv 0$ ):

$$\alpha_{\text{max}}(t, t_{\text{Init}}) = [(t/t_0)^{1/3} - (t_{\text{Init}}/t_0)^{1/3}] . \quad (4)$$

Now, how the metric at  $P$  is affected by a spherical shell of material at coordinate radius  $\alpha$  depends upon the state of clumping there at the appropriate retarded time:  $\Psi[t_{\text{ret}}(t, \alpha)]$ . The total effect is then computed by integrating all shells from  $\alpha = 0$  out to  $\alpha = \alpha_{\text{max}}(t, t_{\text{Init}})$ ; but in order to compute the metric perturbation from each shell quantitatively, it is first necessary to relate this clumping function to an actual physical density of material.

As discussed above, for now consider the  $\Psi(t)$  function as representing the dimensionless ratio of matter which can appropriately be defined as ‘clumped’ at a given time, expressed as a fraction of the total physical density. Assuming a flat MD cosmology as the initially

unperturbed state, the total physical density at all times will merely be an evolved version of the unperturbed FRW critical closure density from early (pre-perturbation) times.

Recalling Equation 2, we have the perturbation term  $[R_{\text{Sch}}(t)/r'] = \{(2GM/c^2)/[r' a_{\text{MD}}(t)]\}$ , with  $a_{\text{MD}}(t) = a_0(t/t_0)^{2/3} \equiv c[18t^2/H_0]^{1/3}$ . The value of  $M$  to use here is given by the clumped matter density at coordinate distance  $\alpha$  times the infinitesimal volume element of the shell. The clumped matter density at time  $t$ , as implied above (and still as considered with respect to the unperturbed background metric), will equal  $[\Psi(t)\rho_{\text{crit}}(t)]$ ; and the volume element in the integrand representing the effects of that shell will be  $4\pi R_{\text{phys}}^2 dR_{\text{phys}} = 4\pi[a_{\text{MD}}(t) \alpha]^2[a_{\text{MD}}(t) d\alpha]$ .

Collecting these terms (and letting  $t' \equiv t_{\text{ret}}(t, \alpha)$ ), the integrand will thus be equal to:

$$[R_{\text{Sch}}(t)/r']_{r'=\alpha \rightarrow (\alpha+d\alpha)} = \{(2G/c^2) dM / [a_{\text{MD}}(t) \alpha]\} \quad (5a)$$

$$= \{(2G/c^2) [a_{\text{MD}}(t) \alpha]^{-1} [\Psi(t') \rho_{\text{crit}}(t)] [4\pi R_{\text{phys}}^2 dR_{\text{phys}}]\} \quad (5b)$$

$$= \{(8\pi G/c^2) \Psi(t') [a_{\text{MD}}(t) \alpha]^{-1} [\rho_{\text{crit}}(t) [a_{\text{MD}}(t)]^3] [\alpha^2 d\alpha]\} \quad (5c)$$

$$= \{(8\pi G/c^2) \Psi(t') a_{\text{MD}}(t)^{-1} [\rho_{\text{crit}}(t_0) a_0^3] [\alpha d\alpha]\} \quad (5d)$$

$$= \{(8\pi G/c^2) \Psi(t') [(t_0/t)^{2/3} (3ct_0)^{-1}] \{[3H_0^2/(8\pi G)] (3ct_0)^3\} [\alpha d\alpha]\} \quad (5e)$$

$$= \{12 \Psi(t') [(t_0/t)^{2/3}] [\alpha d\alpha]\} , \quad (5f)$$

where for simplification we have used  $H_0 = (2/3)t_0^{-1}$  and the fact that  $[\rho(t)a(t)^3]$  is constant, both true for a matter-dominated universe. Note also that only  $\Psi$  is evaluated at the retarded time,  $t_{\text{ret}}(t, \alpha)$ . The *strength* of the metric perturbation (at time  $t$  for point  $P$ ) from a point-like Newtonian perturbation embedded in the expansion actually depends upon its instantaneous physical distance from  $P$  at  $t$ , as is obvious from  $\Phi = \{-GM/[a_{\text{MD}}(t) r]\} \equiv [-GM/R_{\text{phys}}(t)]$  in Equation 1. The only “relativistic” piece of propagating information which is causally delayed is the state of clumping,  $\Psi[t_{\text{ret}}(t, \alpha)]$ , that has just then arrived from coordinate distance  $\alpha$  to observer  $P$  at  $(r, t)$ .

The total integrated metric perturbation function due to clumping,  $I(t)$ , as experienced by a null ray passing through point  $P$  at  $(r, t)$ , is thus calculated via the causal updating integral:

$$I(t) = \int_0^{\alpha_{\text{max}}(t, t_{\text{Init}})} \{12 \Psi[t_{\text{ret}}(t, \alpha)] [(t_0/t)^{2/3}]\} \alpha d\alpha , \quad (6)$$

with  $I(t)$  implicitly being a function of  $t_{\text{Init}}$  (with  $I(t) \equiv 0$  for  $t \leq t_{\text{Init}}$ ), as well as of  $t_0$ .

Inserting this result back into the formalism of Equation 2, the final clumping-perturbed metric that we will use for all of our subsequent cosmological calculations becomes:

$$ds^2 = -c^2[1 - I(t)] dt^2 + \{[a_{\text{MD}}(t)]^2 [1 + (1/3)I(t)]\} |d\vec{r}|^2 . \quad (7)$$

Given this metric, we can define relationships between all of the unperturbed FRW (“bare”) cosmological parameters, and their corresponding observable (“dressed”) parameters. We must first consider cosmological redshifts, where we have:

$$z^{\text{FRW}}(t) \equiv \frac{a_{\text{MD}}(t_0)}{a_{\text{MD}}(t)} - 1 = (t_0/t)^{2/3} - 1, \quad (8)$$

and:

$$z^{\text{Obs}}(t) \equiv \frac{\sqrt{g_{rr}(t_0)}}{\sqrt{g_{rr}(t)}} - 1 = \left[ \sqrt{\frac{1 + (1/3)I(t_0)}{1 + (1/3)I(t)}} (t_0/t)^{2/3} \right] - 1, \quad (9)$$

where quantities without superscripts like  $t_0 \equiv t_0^{\text{FRW}}$ , etc., will generically refer to unperturbed FRW parameters; and where values of observational quantities in our backreaction-perturbed formalism will be expressly indicated (e.g.,  $t_0^{\text{Obs}}$ ).

Now, in order to calculate observed luminosity distances, we must compute the coordinate distance  $r$  of a supernova going off at coordinate time  $t$ , for which a light ray would be arriving here (at  $r = 0$ ) precisely at  $t_0$ . For a null ray and pure inward radial motion we have:

$$r_{\text{SN}}^{\text{FRW}}(t) \equiv |r^{\text{FRW}}(t_0) - r^{\text{FRW}}(t)| = \int_t^{t_0} \left\{ \sqrt{\frac{g_{tt}(t')}{g_{rr}(t')}} \right\} dt' \quad (10a)$$

$$= \int_t^{t_0} \left\{ \frac{c}{a_{\text{MD}}(t')} \sqrt{\frac{1 - I(t')}{1 + (1/3)I(t')}} \right\} dt' \quad (10b)$$

$$= \frac{c}{a_0} \int_t^{t_0} \left\{ (t_0/t')^{2/3} \sqrt{\frac{1 - I(t')}{1 + (1/3)I(t')}} \right\} dt'. \quad (10c)$$

This coordinate distance function can then be converted into an expression for the observed luminosity distance by adapting the expression from the homogeneous FRW case, for which  $d_L = [a_0 r_{\text{SN}} (1 + z)]$ , as follows:

$$d_{\text{L,Pert}}(t) = [a_0 \sqrt{1 + (1/3)I(t_0)}] r_{\text{SN}}^{\text{FRW}}(t) [1 + z^{\text{Obs}}(t)] \quad (11a)$$

$$= \frac{1 + (I_0/3)}{\sqrt{1 + [I(t)/3]}} \frac{c t_0^{4/3}}{t^{2/3}} \int_t^{t_0} \left\{ (t')^{-2/3} \sqrt{\frac{1 - I(t')}{1 + [I(t')/3]}} \right\} dt' \quad (11b)$$

$$= \frac{1 + (I_0/3)}{\sqrt{1 + [I(t_r)/3]}} \frac{c t_0}{t_r^{2/3}} \int_{t_r}^1 \left\{ (t'_r)^{-2/3} \sqrt{\frac{1 - I(t'_r)}{1 + [I(t'_r)/3]}} \right\} dt'_r, \quad (11c)$$

where  $I_0 \equiv I(t_0)$ , and  $t_r, t'_r$  are dimensionless time ratios (e.g.,  $t_r \equiv t/t_0$ ), with no change to the essential form of  $I(t)$  (i.e.,  $I(t) = I(t_r \cdot t_0) \Rightarrow I(t_r)$ ).

All cosmologically-relevant curves, fits, and parameters can now be calculated from the metric (Equation 7), and from this luminosity distance function (Equation 11) and its derivatives, as investigated in BBI. Important modeled quantities include: the residual distance modulus function (with respect to an empty coasting universe),  $\Delta(m - M)_{\text{Pert}}(z^{\text{Obs}})$ , and the quality and probability of its fit,  $\chi_{\text{Fit}}^2$  and  $P_{\text{Fit}}$ , to the Type Ia supernova (SNIa) data; the observed (versus unperturbed) Hubble Constant,  $H_0^{\text{Obs}}$  (versus  $H_0^{\text{FRW}}$ ); the physically-measurable age of the universe,  $t_0^{\text{Obs}}$ ; the “true” value of the total cosmic matter density,  $\Omega_{\text{M}}^{\text{FRW}}$ , which determines the primordial spatial curvature (i.e.,  $\Omega_{\text{M}}^{\text{FRW}} = 1$  for flatness in the pre-perturbed epoch), which our model must relate to some measured value of the density,  $\Omega_{\text{M}}^{\text{Obs}}$ , for normalization (here and in BBI we use  $\Omega_{\text{M}}^{\text{Obs}} = 0.27$ ); the observable values (defined for  $z \rightarrow 0$ ) of the deceleration parameter  $q_0^{\text{Obs}}$ , the effective (total) cosmic equation of state  $w_0^{\text{Obs}}$ , and the jerk parameter  $j_0^{\text{Obs}}$ ; and finally, for comparison with complementary data sets from much earlier cosmic epochs, we compute the acoustic scale of the Cosmic Microwave Background (CMB) acoustic peaks,  $l_{\text{A}}^{\text{Obs}}$ .

As a technical note, we recall that all evolving quantities in our numerical simulation program are calculated as discrete arrays in  $t$  (and in  $z^{\text{Obs}}(t)$ ), with a tested pixelization that is fine enough for great accuracy in all parameters. Given that the discrete version of  $d_{\text{L,Pert}}(z^{\text{Obs}})$  must be differentiated (and evaluated specifically for  $z \rightarrow 0$ ) to obtain cosmological parameters, we do so by using the definition of the derivative for each pixel, as follows:

$$[d_{\text{L,Pert}}^{N'}]_{\{i\}} = \frac{d}{dz^{\text{Obs}}} [d_{\text{L,Pert}}^{(N-1)'}]_{\{i\}} \equiv \frac{d_{\text{L,Pert}}^{(N-1)'}(t_{\{i+1\}}) - d_{\text{L,Pert}}^{(N-1)'}(t_{\{i\}})}{z^{\text{Obs}}(t_{\{i+1\}}) - z^{\text{Obs}}(t_{\{i\}})}, \quad (12)$$

and then obtain the  $z \rightarrow 0$  limit from the last, latest-in-time pixel:

$$[d_{\text{L,Pert}}^{N'}]_{(z \rightarrow 0, t \rightarrow t_0)} \equiv [d_{\text{L,Pert}}^{N'}]_{\{N_{\text{pix}}\}}. \quad (13)$$

The cosmological results which we obtain from this procedure appear to be robust, with only minor difficulties, as will be discussed below; and while the greatest discretization errors occur for  $j_0^{\text{Obs}}$ , which requires three differentiations of  $d_{\text{L,Pert}}(t)$ , virtually all of the results which we quote here for  $j_0^{\text{Obs}}$  should be well within 1% in terms of numerical accuracy.

In order to conduct specific calculations with our formalism, we must design a set of physically reasonable clumping evolution functions,  $\Psi(t)$ , to serve as convenient proxies for the combined effects of the linear density evolution of early-stage clustering, the nonlinear regime and virialization for very dense clumps, and the initial development (in many cases triggered by collisions) of entirely new clumps with substantial mass. Guided by general cosmological considerations and simplicity, in BBI we chose three different classes of time-dependent behaviors to examine:  $\Psi(t) \propto a(t) \propto t^{2/3}$ , which is proportional to the evolving contrast of a density variation,  $\delta\rho/\rho$ , in the linear regime (Kolb & Turner 1990);  $\Psi(t) \propto t$ , a

generally sensible choice depending simply upon the amount of time available for clumping; and  $\Psi(t) \propto t^2$ , an ‘accelerating’ clumping model which we initially chose as a test case to see whether that would possibly help in creating an observed acceleration. This last class of models will take on more significance in this paper, however, since our results below with recursive nonlinearities will force us to regard  $\Psi(t)$  as not merely a simple percentage of clumped versus unclumped matter, but as a quantity reflecting the details of virialization brought to completion (i.e., extremely nonlinear density perturbations) on multiple cosmic scales; and appropriately, the density contrast evolution for inhomogeneities in the nonlinear regime goes as  $\delta\rho/\rho \propto a(t)^n$  with  $n \gtrsim 3$  (Kolb & Turner 1990, p. 322) – that is,  $\delta\rho/\rho \propto t^m$  with  $m \equiv (2/3)n \gtrsim 2$  for a matter-dominated universe.

Quantitatively, we defined our three different classes of clumping evolution models as follows:

$$\Psi_{\text{MD}}(t) \equiv \Psi_0 \left( \frac{t - t_{\text{Init}}}{t_0 - t_{\text{Init}}} \right)^{2/3} \quad (14a)$$

$$\Psi_{\text{Lin}}(t) \equiv \Psi_0 \left( \frac{t - t_{\text{Init}}}{t_0 - t_{\text{Init}}} \right) \quad (14b)$$

$$\Psi_{\text{Sqr}}(t) \equiv \Psi_0 \left( \frac{t - t_{\text{Init}}}{t_0 - t_{\text{Init}}} \right)^2 . \quad (14c)$$

Here  $t_{\text{Init}}$  (or equivalently,  $z_{\text{Init}} = [(t_0/t_{\text{Init}})^{2/3} - 1]$ , as per Equation 8) represents the effective beginning of clumping, such that  $\Psi(t \leq t_{\text{Init}}) \equiv 0$  for all models; and  $\Psi_0 \equiv \Psi(t_0)$  represents the current state of clumping today. Each of these models has two physically meaningful parameters to vary (besides the universally-optimizable parameter for all models,  $H_0^{\text{Obs}}$ ):  $\Psi_0$ , for which we selected values by estimating the fractions of Dark and baryonic matter that may likely be clumped by  $t_0$ ; and  $z_{\text{Init}}$ , for which we selected values by roughly linking the beginning of clumping with the process of cosmic reionization.

In BBI, we evaluated 60 different models, using  $\Psi_0 = (0.78, 0.85, 0.92, 0.96, 1.0)$  and  $z_{\text{Init}} = (5, 10, 15, 25)$  for each of  $\Psi_{\text{Lin}}(t)$ ,  $\Psi_{\text{MD}}(t)$ , and  $\Psi_{\text{Sqr}}(t)$ . We found that these models produced curves which behaved very much like  $\Lambda$ CDM, with the  $\Psi_{\text{Sqr}}$  runs looking like flat  $\Lambda$ CDM with  $\Omega_\Lambda \sim 0.3 - 0.4$ , the  $\Psi_{\text{Lin}}$  runs looking like  $\Omega_\Lambda \sim 0.5 - 0.8$ , and the  $\Psi_{\text{MD}}$  runs looking like  $\Omega_\Lambda \sim 0.65 - 0.97$ .

As was expected, due to the increase in the number of perturbing clumps with distance (as  $r^2$ ), the total perturbative effects were typically dominated by the largest distances (and thus the earliest look-back times) out to which one could still see significant inhomogeneities; hence clumping evolution functions with a more rapid onset of clustering at early times would produce a more powerful causal backreaction effect. Thus the  $\Psi_{\text{MD}}$  models were by far the strongest, while the  $\Psi_{\text{Sqr}}$  models were all too weak to reproduce the observed acceleration,

with the  $\Psi_{\text{Lin}}(t)$  models falling intermediate between the two; and in all cases, the choice of an earlier  $z_{\text{Init}}$  led to a stronger overall backreaction.

All told, roughly a dozen of these models resulted in good fits to the standard candle SNIa data, reproducing the observed cosmic acceleration essentially as well as the best-fit  $\Lambda$ CDM Dark Energy model; and about half of those dozen models produced especially good cosmological parameters, as well. The overall picture was that of a successful attempt at achieving an alternative cosmic concordance without Dark Energy. Additionally, there emerged the bonus of a testable prediction which could distinguish causal backreaction from a Cosmological Constant: a result of  $j_0^{\text{Obs}} \gg 1$  for all of our models which produced good fits, in contrast to the mandatory value of  $j_0^{\text{Obs}} = 1$  for all flat  $\Lambda$ CDM models, regardless of the value of  $\Omega_\Lambda$ .

With those results in hand, the next concern was to determine how the effects of recursive nonlinearities might modify these outcomes, once incorporated into our numerical models. Our initial expectation was that the overall Hubble curves of each modeled cosmology would likely not change significantly, except perhaps at the end, as  $z \rightarrow 0$ ; a result that would not alter the SNIa fitting results much, but which could have a measurable effect upon the cosmological parameters evaluated at  $t_0$  – particularly upon our ‘paradigm falsifiability’ parameter,  $j_0^{\text{Obs}}$ . The actual outcome, however, is that the proper treatment of recursive nonlinearities ends up altering the situation to a great degree, requiring us to re-evaluate (see Section 3) the ultimate implications of causal backreaction; although it does still remain true that an alternative concordance can be successfully achieved with it. First, however, in the following subsection we give the precise details explaining how recursive nonlinearities for causal backreaction are technically implemented in our numerical simulations.

### 2.3. The New Formalism: Incorporating Recursive Nonlinearities into Causal Backreaction

Though in practice necessitating a complete re-write of our numerical simulation program, the essential features of recursive nonlinearities require just two fundamental changes.

The first change involves the rate at which clustering information can propagate through the inhomogeneity-perturbed universe, as depicted earlier in Figure 1. The result is that  $t_{\text{ret}}(t, \alpha)$  and  $\alpha_{\text{max}}(t, t_{\text{Init}})$  are altered from their simple functional forms (as per Equations 3,4) for a matter-dominated FRW universe, and now depend upon the metric perturbation potential function,  $I(t)$ . But as we see from Equation 6,  $I(t)$  is itself calculated via an integral depending upon  $t_{\text{ret}}(t, \alpha)$  and  $\alpha_{\text{max}}(t, t_{\text{Init}})$ . Hence  $I(t)$  is now defined in terms of  $I(t)$ , in a



fundamentally recursive fashion.

Second, the extra spatial volume created by nonzero  $I(t)$  will have a dilution effect upon the strength of the perturbation induced by any (now farther-away) clumped mass upon the metric at our observation point. Examining Equation 5 (specifically 5a), we recall that the perturbation term for each spherical shell of clumped matter is given by  $[R_{\text{Sch}}(t)/r']_{r'=\alpha \rightarrow (\alpha+d\alpha)} = \{(2G/c^2) dM / [a_{\text{MD}}(t) \alpha]\}$ . Now, the differential mass element in the shell,  $dM$ , does not actually change (and therefore requires no correction factor), since the dilution of its mass density is precisely offset by its expanded volume. But what *does* change is the effective distance of those perturbing clumps from the observation point. Recalling that the strength of a Newtonian perturbation embedded in an expanding universe depends simply upon its instantaneous physical distance, we see that the denominator  $[a_{\text{MD}}(t) \alpha]$  must now be replaced by the term:  $[\sqrt{g_{rr}} \alpha] = [a_{\text{MD}}(t) \sqrt{1 + (1/3)I(t)} \alpha]$ , which in the end just puts a factor of  $\sqrt{1 + (1/3)I(t)}$  into the denominator of the integral for  $I(t)$ .

Therefore, the modified formula (replacing Equation 6) for calculating the metric perturbation function  $I(t)$  with the incorporation of recursive nonlinearities (“RNL”), is given as:

$$I^{\text{RNL}}(t) = \int_0^{\alpha_{\text{max}}(t, t_{\text{init}}, I)} \frac{\{12 \Psi[t_{\text{ret}}(t, \alpha, I)] [(t_0/t)^{2/3}]\} \alpha}{\sqrt{1 + (I/3)}} d\alpha, \quad (15)$$

where the term “ $I$ ” inside the integral on the right-hand side represents the actual function,  $I^{\text{RNL}}(t)$ , itself. But since the denominator term is in fact independent of the integration variable  $\alpha$ , we can remove it from the integral and bring it to the left-hand side of the equation. The metric perturbation function can therefore be (numerically) solved for any given  $t$  as the solution of:

$$I^{\text{RNL}}(t) \sqrt{1 + [I^{\text{RNL}}(t)/3]} = \int_0^{\alpha_{\text{max}}(t, t_{\text{init}}, I)} \{12 \Psi[t_{\text{ret}}(t, \alpha, I)] [(t_0/t)^{2/3}]\} \alpha d\alpha. \quad (16)$$

To evaluate the expressions  $t_{\text{ret}}(t, \alpha, I)$  and  $\alpha_{\text{max}}(t, t_{\text{init}}, I)$  in this above integral, we utilize (analogously with the discussion preceding Equations 3,4):

$$\alpha(T, T_{\text{ret}}, I) = \frac{1}{3} \int_{T_{\text{ret}}}^T \frac{\sqrt{1 - I^{\text{RNL}}(T')}}{\sqrt{1 + [I^{\text{RNL}}(T')/3]}} \frac{dT'}{(T')^{2/3}}, \quad (17)$$

with  $T \equiv (t/t_0)$  and  $T_{\text{ret}} \equiv (t_{\text{ret}}/t_0)$ . This expression for  $\alpha(T, T_{\text{ret}}, I)$  could in theory be inverted to produce  $T_{\text{ret}}(T, \alpha, I)$ ; and in addition, we have  $\alpha_{\text{max}} = \alpha(T, T_{\text{init}}, I)$ .

In practice, we perform these recursively-defined ‘integrals’ by utilizing discrete arrays in cosmic coordinate time with some large number of pixels covering the range from  $T_{\text{init}}$  to  $T_0 \equiv 1$ , for which the later pixels are calculated in terms of the earlier pixels. Beginning

with the first pixel at  $T_{\text{Init}}$ , we thus have the recipe (with  $N_{\text{pix}}$  pixels, and  $\Delta T = [(T_0 - T_{\text{Init}})/(N_{\text{pix}} - 1)]$ ):

$$\alpha_{\text{max},1} = I_1^{\text{RNL}} \equiv 0, \quad (18a)$$

$$\alpha_{\text{max},2} = \frac{1}{3} \frac{\Delta T}{T_{\text{Init}}^{2/3}}, \quad I_2^{\text{RNL}} = 0, \quad (18b)$$

and then, for  $i = \{3, N_{\text{pix}}\}$ :

$$\alpha_{\text{max},i} = \alpha_{\text{max},(i-1)} + \left\{ \frac{1}{3} \frac{\sqrt{1 - I_{(i-1)}^{\text{RNL}}}}{\sqrt{1 + [I_{(i-1)}^{\text{RNL}}/3]}} \frac{\Delta T}{[T_{(i-1)}]^{2/3}} \right\}, \quad (19a)$$

$$X_i^{\text{RNL}} = \frac{12}{T_i^{2/3}} \sum_{k=\{1,(i-2)\}} \{ \Psi[T_{(i-k)}][\alpha_{\text{max},i} - \alpha_{\text{max},(i-k)}][\alpha_{\text{max},(i+1-k)} - \alpha_{\text{max},(i-k)}] \} \quad (19b)$$

$$I_i^{\text{RNL}} \sqrt{1 + [I_i^{\text{RNL}}/3]} = X_i^{\text{RNL}}. \quad (19c)$$

The result of this iterative loop is the discrete array  $\{I_i^{\text{RNL}}\}$ , which serves as  $I^{\text{RNL}}(t)$  for all cosmological calculations, as described above. As a test, we have verified that removing the effects of recursive nonlinearities (essentially adjusting to unity all terms inside the radical signs in Equations 19a,c) succeeds in reproducing the results of our old formalism to a great degree of accuracy; and for our new model simulations with the recursive nonlinearities included, we have checked to make sure that the full suite of results with this new formalism appears quite sensible and consistent in all cases.

We have also tested the pixelization for precision of the output results, finding that runs with  $\sim 1000$  pixels are sufficient for quick model parameter optimization searches, producing all cosmological results to within a couple percent of their ‘true’ values (i.e., the values to which the parameters asymptote for much larger pixelizations); and that going to  $\sim 5000 - 10000$  pixels yields cosmological output results that are stable to within a small fraction of a percent. (Though going all the way to  $\sim 25000$  pixels actually leads to discretization problems due to round-off error, which causes problems for higher derivatives of the luminosity distance function, leading to instability in the value of  $j_0^{\text{Obs}}$ ; and so we avoid pixelizations this large.) Our high-precision output cosmological parameters – i.e., all numerical results other than those from optimization searches – which we will quote in Section 3, below, have all been obtained from runs with  $\sim 5000 - 10000$  pixels (not counting the further addition of a smaller number ( $\sim 1000$ ) of extra pixels used for integrating the Hubble curves out to the computationally simpler region past  $z_{\text{Init}}$ , before the simulated onset of clumping).

### 3. RESULTS WITH RECURSIVE NONLINEARITIES

#### 3.1. Weakened Backreaction Effects: Difficulties with “Clumping-Saturated” Models

As mentioned previously, the incorporation of recursive nonlinearities (henceforth RNL) does not merely affect the late-time behavior as  $z \rightarrow 0$ , but in fact exerts a profound damping influence upon the entire process of causal backreaction, weakening the overall effect for a given set of model input parameters. As an example, we consider the impact of RNL upon one of the best-fitting models from BBI,  $\Psi_{\text{Lin}}(t)$  with  $z_{\text{Init}} = 25$  and  $\Psi_0 = 1.0$ . As depicted in Figure 2, we see that adjusting the simulations to include RNL greatly reduces the apparent acceleration effect – no longer quite even achieving an ‘acceleration’, in fact, since  $q_0^{\text{Obs}} = 0.058 > 0$ .

For ease of comparison to the results from BBI, in this paper we will still primarily use the SNIa data from the SCP Union1 supernova compilation (Kowalski et al. 2008) for conducting fits of our new models with RNL. As would be expected from Figure 2, the new fit to these SNIa data (not shown here), even after re-optimization with respect to  $H_0^{\text{Obs}}$ , is much worse in this modified model, with its ‘chi-squared’ value – for 307 SNIa minus 3 model parameters yielding 304 degrees of freedom – increasing from  $\chi_{\text{Fit}}^2 = 312.1$  without RNL, to  $\chi_{\text{Fit}}^2 = 410.1$  with it (where for comparison,  $\chi_{\text{Fit}}^2 = 311.9$  for best-fit flat  $\Lambda$ CDM). Visually speaking, though this causal backreaction model with RNL does at least manage to clearly separate itself from the strongly decelerating behavior of matter-only flat SCDM, it no longer matches best-fit  $\Lambda$ CDM but now falls significantly short of it, lying somewhere in the middle between SCDM and  $\Lambda$ CDM; and correspondingly, the output cosmological parameters – though still being substantially modified from those for the unperturbed case without causal backreaction – are now far less reflective of those required for a successful concordance, as would indeed be expected from a cosmological model producing too weak of an ‘acceleration’ effect.

Within the set of 60 model input parameter choices from BBI (all with  $\Psi_0 \leq 1$ ), the ‘best’ models now, with RNL included, are  $\Psi_{\text{MD}}$  with  $(z_{\text{Init}}, \Psi_0) = (5, 1.0)$ , which fits the SNIa most successfully with  $\chi_{\text{Fit}}^2 = 397.4$ ; and  $\Psi_{\text{Sqr}}$ , also with  $(z_{\text{Init}}, \Psi_0) = (5, 1.0)$ , which despite yielding a worse overall fit ( $\chi_{\text{Fit}}^2 = 421.3$ ) because of too little clumping at early times, manages to produce the largest late-time backreaction effect, achieving an actual ‘acceleration’ with  $q_0^{\text{Obs}} = -0.026 < 0$ . These two models are plotted in Figure 3, shown along with matter-only flat SCDM and  $\Lambda$ CDM, where all models are now shown in the figure as optimized with respect to  $H_0^{\text{Obs}}$  for the Union1 SNIa data set.

One of the most important changes in causal backreaction due to RNL, is the slow-

down that it causes for inhomogeneity information propagating in from great cosmological distances. This strongly damps the backreaction effects due to perturbations at the outer edges of an observer’s causal inhomogeneity horizon, which despite being the most distant ones are nevertheless very important for backreaction because they include the largest spherical shells of inhomogeneous matter, containing the greatest incremental mass (per shell) of perturbations overall.

Besides simply weakening the total backreaction effect, RNL acts specifically to inhibit the contributions from older perturbations generated during relatively early clumping epochs, due to a reduction of the coordinate distance (and thus of the volume of clumped matter now enclosed by the sphere) out to some given propagative look-back time; an inhibition that is particularly strong if the perturbation potential  $I(t)$  has grown too close to unity very early on. One important potential result is that this may significantly lessen the ongoing effects of causal backreaction into the far future – due in the pre-RNL formalism to eternally-expanding observational horizons – an issue related to the ultimate possible fates of the universe, to be discussed further in Section 3.4, below. But our immediate concern here is to note that RNL makes later (i.e., more recently generated) clumping far more effective than earlier clumping in terms of generating a late-time acceleration. Hence in our runs here with RNL, we obtain the strongest apparent acceleration effects with the  $\Psi_{\text{Sqr}}$  models, and the weakest with the  $\Psi_{\text{MD}}$  models; also, choosing smaller (i.e., later) values of  $z_{\text{Init}}$  always makes  $q_0^{\text{Obs}}$  more ‘accelerative’ (smaller or more negative), as well. This is all very different from the results in BBI, where the  $\Psi_{\text{Sqr}}$  functions were by far the weakest models at producing an apparent acceleration; and where the  $\Psi_{\text{MD}}$  models were so strong that small or mid-range values of  $z_{\text{Init}}$  were necessary to obtain good fits, since those models with the beginning of clumping occurring significantly *earlier* than  $z_{\text{Init}} \sim 5$  led to an actual overkill of acceleration.

This behavior of causal backreaction with RNL suggests that we may be able to get a stronger accelerative effect by using later and later (i.e., smaller) values of  $z_{\text{Init}}$ ; and indeed, going from  $z_{\text{Init}} = 5$  to  $z_{\text{Init}} = 2$  for the  $\Psi_{\text{Sqr}}$  model with  $\Psi_0 = 1.0$  does strengthen the observed acceleration from  $q_0^{\text{Obs}} = -0.026$  to  $q_0^{\text{Obs}} = -0.043$ . But this type of procedure does not save these models as a mechanism for explaining the apparent acceleration, due to several obvious problems. First of all, the total amount of generated acceleration is still far too small, and thus the fits to the SNIa data remain extremely poor (and in fact,  $\chi_{\text{Fit}}^2$  gets *worse* for the  $\Psi_{\text{Sqr}}$  runs with later  $z_{\text{Init}}$ ). Besides such problems with the SNIa fits, the output cosmological parameters are also unacceptable for such runs, with quantities like  $t_0^{\text{Obs}}$  and  $\Omega_{\text{M}}^{\text{FRW}}$  growing far too small with decreasing  $z_{\text{Init}}$ , thus spoiling any efforts at achieving an alternative cosmic concordance. Lastly, such input parameters do not even make good physical sense – can we seriously estimate the effective onset of cosmic clustering as beginning at  $z_{\text{Init}} \sim 2$ , or even later? Clearly, we cannot achieve our goals of reproducing the observed

cosmic evolution with causal backreaction in the presence of RNL while stuck within the confines of models with  $\Psi_0 \leq 1.0$ .

These difficulties lead us to the question of what may be wrong with our formalism; a question to which there are several possible answers.

First of all, it is certainly possible that causal backreaction is not the mechanism fundamentally responsible for the observed cosmic acceleration. Even so, given that these effects are (as we argue) real and significant – the cosmic expansion is clearly different than it would be without them, as we have seen above in Figures 2 and 3, witnessing the clear separation between our models and unperturbed  $\Lambda$ CDM – even a cosmology actually dominated by some form of Dark Energy would be strongly modified by causal backreaction, leading to misconceptions about the evolution of the universe (and about the nature of that Dark Energy, itself) were these effects not taken into account. Alternatively, causal backreaction may be part of a ‘combination’ solution for explaining the apparent acceleration – in conjunction, perhaps, with observational effects (recall Section 2.1) such as lensing or other inhomogeneity-induced perturbations to the luminosity distance function  $d_L(z)$  – such that the *total* result from all perturbative effects, combined, may be sufficient to remove the need for Dark Energy.

Another possibility is that our fundamental physical approach towards causal backreaction is far too oversimplified to properly model the cosmic evolution, just as we have argued was true for the standard (non-causal) method traditionally used for estimating backreaction. There are many possible flaws with our approach – for example, perhaps the linearized McVittie solution (from which we calculated our perturbative metric in Section 2.2) is inappropriate, given that the total mass of the perturbation in that metric is fixed as constant in time (Kaloper et al. 2010), in contrast to the tendency of overdensities in the real universe to keep increasing in mass due to incoming mass flows. (Though our growing  $\Psi(t)$  functions are of course intended as an alternative way of accounting for this.) On the other hand, it is quite possible that the complex processes of cosmic structure formation are too dynamically rich to be modeled accurately by a Newtonian-perturbed metric containing just a single perturbation potential function. The very natures of our  $\Psi(t)$  functions are obviously oversimplified – not accounting at all, for example, for the differences between the simple linear evolution of matter overdensities, and the far more complex process of nonlinear density perturbation evolution – the latter including subsidiary effects such as virialization and stabilization (the detailed time-dependence of which may be quite important, though our formalism completely neglects it), as well as “gastrophysics” feedback (e.g., energy injection from star formation and from the supernovae, themselves) resulting in baryon shock heating, and so on. Considering such complications, it is possible that no simple functional form of

*any* kind for  $\Psi(t)$  – and for that matter, no simple numbers for  $z_{\text{Init}}$  or  $\Psi_0$  – may suffice for a realistic description of the physics. Perhaps nothing would be accurate short of a fully-detailed cosmic simulation program, calculating a realistically self-consistent representation of the intertwined behaviors of cosmic structure formation and astrophysical feedback processes as they evolve together over time.

A different, possibly significant flaw may be our complete neglect of *gravitational* nonlinearities; after all, values for the ‘Newtonian’ perturbation potential in the range of  $I_0 \sim 0.2 - 0.6$  are certainly not negligible, and may imply higher-order gravitational terms from general relativity that would contribute significant backreaction effects for any reasonable model of the evolution of cosmic structure. Leaving out such nonlinear gravitational terms may imply that our calculations here are not serving as an ‘estimate’ of the overall causal backreaction effect, but rather as a *lower limit* to it.

Yet another possibility is that the greatly simplifying assumption of a smoothly-inhomogeneous universe is incompatible with a proper treatment of recursive nonlinearities; after all, inhomogeneities massive on a truly cosmological scale, such as galaxy clusters, are not smoothly spread in angle, but are concentrated at particular locations on the sky. As such, RNL effects would slow down the propagation of inhomogeneity information more strongly along some directions than along others; and so perturbative effects from new clumps, located in new directions, may be able to ‘slip in’ with less delay than would inhomogeneity information coming in from the same directions on the sky as pre-existing clusters that have already imposed their causal backreaction effects upon us. (A kind of *cosmic* “channeling” effect, so to speak.) But quantitatively significant or not, it is likely that such issues cannot be properly evaluated without the development of a fully-3D simulation program for causal backreaction, as discussed previously in Section 2.1.

On the other hand, the main difficulty here may really be much simpler: the basic physical assumptions and methods of our formalism might actually be capable of modeling causal backreaction effects well enough, with the problem simply being inadequate choices for our (heuristically-adopted) clumping evolution models and model input parameters. Given the above results with RNL, it is clear that simply tweaking the detailed time-dependence of the  $\Psi(t)$  functions would not be enough to obtain good data fits; but despite such difficulties, there is actually one very simple thing that we *can* do, which may extend the applicability of our causal backreaction simulation formalism, while also dealing with some very real physical effects in an empirical yet useful way. From the results in this section, it is clear that we cannot achieve a new cosmic concordance with what one might call “clumping-saturated” models that are ultimately limited in strength to values of  $\Psi_0$  bounded above by unity. But what about models with  $\Psi_0 > 1$ ? Such models would clearly lead to much stronger backre-

action effects (with no pre-determined upper bound, obviously), and could perhaps include models that explain all cosmological observations, re-establishing an alternative concordance for causal backreaction even in spite of the damping effects of RNL. Given our basic definition of  $\Psi_0$  as “the fraction of cosmic matter in the clumped, self-stabilized state”, one may ask whether it is ever physically appropriate to use values of  $\Psi_0$  in excess of unity. In the upcoming section, we will argue that the answer is *yes*, that it is entirely appropriate – and in fact, both useful and necessary – for a valid phenomenological description of *hierarchical clustering* in the universe.

### 3.2. Strengthened Backreaction Effects: Regaining an Observed Acceleration with Hierarchical, Nonlinear Clustering

The convenient but ad-hoc representation of the state of cosmic clumping at some given time  $t$  with just a single number –  $\Psi(t)$  – is clearly an extreme simplification, as discussed above. Even aside from our neglect of the detailed time dependence of virialization processes by having this function simply represent the clumped matter fraction over time, there is also the fact that large-scale structure is not a featureless blob: the ‘clumped’ state is not a simple binary state, ‘on’ or ‘off’. Most notably, clustering in the universe is not structure-free, but instead exhibits a roughly discrete form of hierarchical clustering, with identifiable structures existing on a few well-defined scales – for example, galaxies existing as virialized groupings of stars, galactic clusters as virialized groupings of galaxies, and so on. This recognizable substructure will obviously affect the resulting causal backreaction that is induced, and so the question becomes how to best (and most simply) estimate the effects of such substructure.

One conclusion which we can immediately draw is that clustering with multiple levels of substructure will exert *more* of a total backreaction effect than would a simpler form of structure without them. From elementary physical considerations, it is clear that the total gravitational potential energy contained within a bound collection of individually-condensed clumps will be larger in magnitude (i.e., more negative) than that within a bound volume of featureless dust. By the Virial Theorem, the presence of a greater amount of (negative) potential energy requires the counterbalance of more kinetic energy, which implies more backreaction-causing vorticity and velocity dispersion. Thus the existence of more (stable) substructure implies that more induced causal backreaction was generated during the process of stabilizing it.

But one must ask, how much more? Each distinct level of structure actually involves the *same* amount of mass, when considering it over a fixed cosmic volume – whether one considers the individual virializations of the tens or hundreds of galaxy clusters in a single

supercluster, or of the tens or hundreds of *thousands* of individual galaxies in that same supercluster, or of the trillions of stellar-mass bodies in that supercluster – and in virializing the same amount of mass, it seems reasonable to expect the same amount of volume-generating velocity dispersion to occur. Thus we claim that an effective phenomenological way of estimating the total backreaction effect that has been generated by a stabilized volume of mass with multiple levels of internal substructure on different length scales, is by *counting the effective number of levels of structure* that have attained an essentially complete virialization. Astrophysically realistic structure formation therefore provides a natural way in which  $\Psi(t)$  should be expected to not only reach but to eventually exceed unity, and then to even keep growing (without any fundamental theoretical limit) as long as there are new levels of structure to be brought into a self-stabilized state.

To avoid giving ourselves an infinite amount of leeway in searching for an alternative concordance, however, it is important to place bounds upon the ‘reasonable’ values of  $\Psi(t_0) \equiv \Psi_0$  that one should expect to find when using causal backreaction to explain the apparent acceleration. The essence of the question is simple: “How many levels?” In particular, we need only consider those typical length scales which became virialized during or not too long before the general cosmic time of the observed acceleration (i.e.,  $z \lesssim \text{few}$ ), since (as will be shown in Section 3.3) RNL sharply limits the ongoing influence of causal backreaction effects from relatively early, ‘outdated’ virializations (*especially* when they are strong).

It seems safe to include at least two scales in our  $\Psi_0$  estimate: that of individual galaxies, and that of galaxy clusters, implying a  $\Psi_0$  of at least 2. Going below these classes of structures in length scale, there are of course a multitude of individual star clusters and solar systems (supported by the vorticity in their orbital motions) that have not too long ago undergone (or are still undergoing) relaxation; and even below that in scale, there are continual generations of newly-forming solid objects supported by internal body forces (which going beyond the perfect-fluid approximation, also contribute positive terms to the Raychaudhuri equation). Below this, of course, there is infinite regress; though at some point it becomes absurd to consider ever-smaller structures, and significant quantities of new self-stabilization is not happening at very small scales in any case. It is difficult to precisely estimate the total effective causal backreaction feedback that is induced by structures at sub-galaxy scales; but for our purposes, let us consider it a ‘significant fraction’ of 1.

At much higher scales, there are groupings of galactic clusters, leading to superclusters, and the largest known structures in general. Superclusters are too large to be gravitationally bound yet (and certainly were not bound at high redshifts, back around the onset of the apparent acceleration), but are experiencing relaxation processes that are underway during the current epoch. Once again lacking a precise estimate, we hypothesize that the contribu-



tions by stabilized structure formation to backreaction from scales larger than that of typical galaxy clusters, in terms of increasing the effective value of  $\Psi_0$ , may amount to a small but non-negligible fraction of 1.

All told, reasonable values of the present-day clumping evolution parameter for causal backreaction, when one considers hierarchical clustering, may be within the range  $\Psi_0 \sim 2-3$ ; or really pushing it, perhaps within  $\Psi_0 \sim 2-4$ . Allowing ourselves such an enhanced phase space for  $\Psi_0$ , the question then becomes whether or not we can re-establish causal backreaction, now with RNL included, as a successful (and ‘concordant’) explanation of the observed acceleration.

For each of the  $\Psi_{\text{MD}}$ ,  $\Psi_{\text{Lin}}$ , and  $\Psi_{\text{Sqr}}$  clumping evolution functions, different values of  $z_{\text{Init}}$  can be explored, where the highest reasonable value (say,  $z_{\text{Init}} \sim 25$ ) is set to represent a time shortly before the onset of cosmic reionization; and where the smallest reasonable value (say,  $z_{\text{Init}} \sim 2$ ) would represent the time leading up to serious and intense virialization, signaled by such events as the supernovae themselves (noting that the highest-redshift SNIa in compilations like those of the SCP Union collaboration tend to be at  $z \sim 1.5$  or so). Then for each value of  $z_{\text{Init}}$  that we adopt, a search is done over  $\Psi_0$  to find which value achieves a best-fit by minimizing  $\chi_{\text{Fit}}^2$ .

Finding a value of  $\Psi_0$  which minimizes  $\chi_{\text{Fit}}^2$  for any given  $z_{\text{Init}}$  can always be done – and often with good results, where the  $\chi_{\text{Fit}}^2$  value is almost as low (and sometimes even lower) than that for the best-fit  $\Lambda$ CDM model. But there is more to the true task of ‘optimization’ than this, since besides achieving a good fit to the SNIa data, one must also match the observed values of a variety of complementary cosmological parameters in order to produce a proper alternative concordance. Achieving all of these goals simultaneously is more challenging; and so to conveniently measure our ability in this regard, we define what can roughly be considered an “Average Percent Deviation from Concordance” parameter, as follows:

$$\begin{aligned} \text{Avg. \% Dev.} = & \frac{1}{6} \left\{ \frac{|\Omega_{\text{M}}^{\text{FRW}} - 1|}{1} + \frac{|H_0^{\text{Obs}} - 69.96|}{69.96} + \frac{|t_0^{\text{Obs}} - 13.64|}{13.64} \right. \\ & \left. + \frac{|w_0^{\text{Obs}} - (-0.713)|}{|-0.713|} + \frac{|l_{\text{A}}^{\text{Obs}} - 285.4|}{285.4} + \frac{(\chi_{\text{Fit}}^2 - 311.9)}{311.9} \right\} \times 100\% , \quad (20) \end{aligned}$$

where all of the numerical values used above to represent the ‘Concordance’ values are reference numbers obtained from the Union1-best-fit flat  $\Lambda$ CDM model (i.e.,  $\Omega_{\Lambda} = 0.713$ ,  $H_0 = 69.96 \text{ km s}^{-1}\text{Mpc}^{-1}$ , with the approximation of zero cosmological radiation density), and all quantities are expressed here in typical units (e.g., GYr for  $t_0^{\text{Obs}}$ ).

An optimization search over the range of reasonable input parameters for our three cluster evolution functions, using quick simulation runs (i.e., 1000 pixels for  $t \geq t_{\text{Init}}$ ), produces a number of models that provide both good SNIa fits and good output cosmological

parameters. A summary of the results of this search – here showing only those runs which possess the optimal  $\Psi_{0,\text{Opt}}$  value for minimizing  $\chi_{\text{Fit}}^2$  in each particular  $z_{\text{Init}}$  case – is given in Table 1.

We see that the best (minimized) value of  $\chi_{\text{Fit}}^2$  obtainable is in fact somewhat different for different choices of the input parameter  $z_{\text{Init}}$ ; but varying even more dramatically with  $z_{\text{Init}}$  is the average deviation from Concordance for its  $\chi_{\text{Fit}}^2$ -minimizing run. We have highlighted (in bold) five of the cases in Table 1:  $\Psi_{\text{MD}}$  with  $(z_{\text{Init}}, \Psi_0) = (1.5, 2.8)$  and  $(z_{\text{Init}}, \Psi_0) = (2, 2.9)$ ;  $\Psi_{\text{Lin}}$  with  $(z_{\text{Init}}, \Psi_0) = (2, 3.2)$  and  $(z_{\text{Init}}, \Psi_0) = (3, 3.3)$ ; and  $\Psi_{\text{Sqr}}$  with  $(z_{\text{Init}}, \Psi_0) = (25, 4.1)$ . We will refer to these cases as ‘best runs’, chosen not by the global minimization of  $\chi_{\text{Fit}}^2$ , but by selecting  $z_{\text{Init}}$  settings for which the  $\chi_{\text{Fit}}^2$ -minimizing  $\Psi_{0,\text{Opt}}$  run produces cosmological parameters with very small deviations from Concordance, in addition to having values of  $\chi_{\text{Fit}}^2$  that are acceptably close to the smallest ones found for the relevant  $\Psi(t)$  function. We will consider the astrophysical implications of the particular  $(z_{\text{Init}}, \Psi_{0,\text{Opt}})$  input values required to obtain these ‘best’ runs, later on, below; but first, we consider here the principal output results of interest.

These five best runs (now re-done with 10000 pixels each, for higher precision) are all good fits to the SNIa data, as can be seen from their  $\chi_{\text{Fit}}^2$  values, which are nearly as small as that for the best-fit  $\Lambda\text{CDM}$  model (and are even smaller than that from  $\Lambda\text{CDM}$  for *all* of the  $\Psi_{\text{Sqr}}$  runs in the table). The high quality of these fits can also be inferred from Figure 4, where we plot three of these runs – one each for  $\Psi_{\text{MD}}$ ,  $\Psi_{\text{Lin}}$ , and  $\Psi_{\text{Sqr}}$  – against  $\Lambda\text{CDM}$  and the matter-only flat SCDM model, showing our runs to be very good at mimicking best-fit  $\Lambda\text{CDM}$  (particularly within the redshift region  $z \lesssim 1$ , containing most of the SNIa), thus demonstrating their ability to successfully reproduce the cosmic ‘acceleration’ as it is actually observed.

The derived output parameters for these five best  $\Psi_0 > 1$  runs are presented in Table 2. Here we see how their  $\chi_{\text{Fit}}^2$  values, nearly as good or (for  $\Psi_{\text{Sqr}}$ ) better than that for best-fit  $\Lambda\text{CDM}$ , makes them comparable to  $\Lambda\text{CDM}$  in terms of the fit probability,  $P_{\text{Fit}}$  (noting that  $\Lambda\text{CDM}$  has fewer optimizable model parameters, and thus more degrees of freedom, giving it a higher  $P_{\text{Fit}}$  value for the same  $\chi_{\text{Fit}}^2$ ). We also see that their present-day ‘Newtonian’ perturbation values,  $I_0 \equiv I^{\text{RNL}}(t_0)$ , do not go much higher than  $I_0 \sim 0.6$ ; this places moderate limits upon the effects of gravitational nonlinearities – which are *not* explicitly dealt with in our formalism – implying at least some reasonable level of accuracy for our models regarding this approximation.

Considering the observational cosmological parameters, there is an astrophysically-interesting modification of  $z^{\text{Obs}}$  (relative to  $z^{\text{FRW}} = 1$ ) of  $\sim 14 - 17\%$ ; while the best-fit observable Hubble constant,  $H_0^{\text{Obs}}$ , is in all cases extremely close (well within 1%) of the

$\Lambda$ CDM Concordance value of  $69.96 \text{ km s}^{-1}\text{Mpc}^{-1}$ . The cosmic ages of these models are all at least equal to the “Concordance” value of  $t_0^{\text{Obs}} = 13.64 \text{ GYr}$  (with the  $\Psi_{\text{Sqr}}$  run being *exactly* equal to it); and since cosmologies with higher (if still reasonable) ages would also solve the Cosmic Age Problem just as well, all of these runs (no more than  $\sim 0.8 \text{ GYr}$  older) therefore appear to have quite acceptable values of  $t_0^{\text{Obs}}$ .

The goal of achieving spatial flatness without Dark Energy is also accomplished quite successfully, with  $\Omega_{\text{M}}^{\text{FRW}} \sim 0.94 - 1.16$ . This result is even more impressive given the fact that to produce these numbers, one must first normalize the calculations to some pre-specified value of the observed matter density,  $\Omega_{\text{M}}^{\text{Obs}}$ ; and thus any uncertainties in that observed density will translate themselves into error bars on the  $\Omega_{\text{M}}^{\text{FRW}}$  values output from the simulations – and with a factor *greater* than unity, since  $\Delta\Omega_{\text{M}}^{\text{FRW}} \simeq \Delta\Omega_{\text{M}}^{\text{Obs}} (\Omega_{\text{M}}^{\text{FRW}} / \Omega_{\text{M}}^{\text{Obs}}) \sim \Delta\Omega_{\text{M}}^{\text{Obs}} (1 / \Omega_{\text{M}}^{\text{Obs}}) \sim (3 - 4) \times \Delta\Omega_{\text{M}}^{\text{Obs}}$ . For all of the results presented in this paper, we have used  $\Omega_{\text{M}}^{\text{Obs}} \equiv 0.27$ . If one assumes that this value is more likely to be too high than too low, then models here with results of  $\Omega_{\text{M}}^{\text{FRW}} \gtrsim 1.0$  would be somewhat better than those with  $\Omega_{\text{M}}^{\text{FRW}} \lesssim 1.0$ ; but in any case, all of the models in Table 2 are clearly successful at effectively achieving flatness.

In terms of providing a sufficient (apparent) acceleration, these models are again successful, with  $w_0^{\text{Obs}} \sim (-0.64) - (-0.75)$ , effectively bracketing the Concordance value of  $w_0^{\text{Obs}} = -0.713$ . We also note that since the precise cosmological parameters obtained from SNIa fits are highly model-dependent (e.g., Cattoën & Visser 2008), it is therefore not necessary for alternative-cosmology models to *exactly* reproduce the  $w_0^{\text{Obs}}$  result from Concordance  $\Lambda$ CDM, but merely to generate an ‘accelerative’ value of  $w_0^{\text{Obs}}$  strong enough to provide a sufficiently good fit to the supernova data, as has been done here.

One final quantity of great importance to be reproduced by an alternative concordance is the CMB acoustic scale,  $l_{\text{A}}^{\text{Obs}}$  – a cosmological parameter that weighs the cosmic evolution over vast distances in space and time. We see here that for the Concordance value of  $l_{\text{A}}^{\text{Obs}} = 285.4$  (as computed using a toy  $\Lambda$ CDM model with no radiation), excellent matches are achieved by  $\Psi_{\text{MD}}$  with  $(z_{\text{Init}}, \Psi_0) = (2, 2.9)$ , and  $\Psi_{\text{Lin}}$  with  $(z_{\text{Init}}, \Psi_0) = (3, 3.3)$  (which is why we chose these  $\Psi_{\text{MD}}$  and  $\Psi_{\text{Lin}}$  models to show in Figure 4 over the other highlighted ones in Table 1, despite their slightly worse  $\chi_{\text{Fit}}^2$  values); and sufficiently good matches are obtained by the remaining three models in Table 2. Although a discrepancy of  $\Delta l_{\text{A}}^{\text{Obs}} \sim 10$  with respect to the value expected from  $\Lambda$ CDM Concordance is certainly something that would be noticeable from observations, we will see later on (in Section 3.3) that one can do even better than this with more refined models (for the  $\Psi_{\text{Sqr}}$  case, particularly).

The last remaining output parameter quoted in Table 2 is the “jerk” or “jolt” parameter,  $j_0^{\text{Obs}}$ . As discussed at length in BBI, rather than serving as a well-observed cosmological

parameter to be matched by theories aiming for an alternative concordance, the (still poorly-measured) value of  $j_0^{\text{Obs}}$  can be viewed as a *prediction* of one’s theory, useful for ultimately distinguishing such theories from Cosmological Constant Dark Energy (since flat  $\Lambda$ CDM is always constrained to  $j_0 = 1$ , for *any* value of  $\Omega_\Lambda = 1 - \Omega_M$ ). We recall that the old version of our causal backreaction simulation program, without RNL, obtained a set of best-fit models which all possessed very high values of the jerk parameter – specifically,  $j_0 \sim 2.6 - 3.8$  for the half-dozen best runs – providing a clear and distinct way of observationally distinguishing our causal backreaction paradigm from a Cosmological Constant, or from any other slowly-evolving form of Dark Energy reasonably close to  $\Lambda$ CDM. But here the results in Table 2 show that when RNL is properly incorporated into our formalism, the situation becomes far less clear: the best-fitting  $\Psi_{\text{MD}}$  and  $\Psi_{\text{Lin}}$  models now prefer *low* values of the jerk parameter ( $j_0^{\text{Obs}} \sim 0.5 - 0.6$  and  $j_0^{\text{Obs}} \sim 0.8 - 0.9$ , respectively); and the best-fit  $\Psi_{\text{Sqr}}$  model, though still predicting a value higher than unity, now only goes so high as  $j_0^{\text{Obs}} \sim 1.7$ . A further analysis below in Section 3.3 will demonstrate that even this result may be subject to substantial change; and thus the search for a reliable observational method for ‘falsifying’ our causal backreaction paradigm (that is, materially distinguishing it from  $\Lambda$ CDM) will likely be more difficult than what was hoped for in BBI, where the possible impact of recursive nonlinearities was still only dealt with in terms of qualitative caveats.

With this analysis of our ‘output’ results done, we now look at the *input* parameters which were necessary to produce these good cosmological fits. First of all, considering  $z_{\text{Init}}$ , we see from Table 1 that to obtain good cosmological output parameters from the  $\Psi_{\text{MD}}$  and  $\Psi_{\text{Lin}}$  models, we have had to impose an *extremely late* value for the time representing the ‘beginning’ of structure formation – specifically,  $z_{\text{Init}} \sim 1.5 - 3$ . This is a direct result of the effects of RNL, which for an already-perturbed universe will slow down the continued propagation of old perturbations coming in from great cosmological distances, thus rendering the causal backreaction contributions of early-developing inhomogeneities to the late-time ‘acceleration’ much weaker than they were for the equivalent models simulated in BBI. This is a serious problem for the  $\Psi_{\text{Lin}}$  and (even more so) for the  $\Psi_{\text{MD}}$  functions, which are especially designed to provide more early clustering, at the expense of late-time clustering. We must ask, in fact, whether input values like these for  $z_{\text{Init}}$  even make astrophysical sense, given the fact that  $z^{\text{Obs}} \sim 3$  actually marks the epoch during which the large-scale collapse of material and the resulting galactic feedback (from star formation, etc.) begins acting strongly to shock-heat cosmic baryons, sending a significant portion of the baryons into the superheated IGM (e.g., Cen & Ostriker 2006), thus helping to *slow down* further structure formation.

This problem goes away, however, for the  $\Psi_{\text{Sqr}}$  runs, which have enough late-time clumping to remove the need for choosing a late (i.e., small) value of  $z_{\text{Init}}$  to get good output cos-

mological parameters. The runs only get better, in fact, as one goes to higher  $z_{\text{Init}}$ , and we stop at  $z_{\text{Init}} = 25$  not because optimization tells us to (though increasingly early initialization times eventually brings diminishing returns), but because it is not physically reasonable to set the start of clustering too long before the onset of reionization.

Besides this success of providing an alternative concordance with reasonable  $z_{\text{Init}}$  values, some reflection shows that the  $\Psi_{\text{Sqr}}$  runs are the most sensible in every regard. As we now consider the  $\Psi(t)$  function to represent the feedback effects of completed clustering on several different, dynamically-defined scales in hierarchical structure formation – rather than as a simple percentage of ‘clumped’ versus ‘unclumped’ matter – the causal backreaction process becomes more naturally focused upon structure formation in the highly nonlinear regime of density perturbations. And as we recall from above, density fluctuations in the nonlinear regime evolve as  $\delta\rho/\rho \propto t^m$  with  $m \gtrsim 2$  for a matter-dominated universe, meaning that  $\Psi(t)$  functions evolving as  $\Psi_{\text{Sqr}} \propto t^2$  (or functions growing with even larger powers of  $t$ ) are therefore the most relevant models for causal backreaction, rather than those with smaller powers of  $t$  like the  $\Psi_{\text{Lin}}$  or  $\Psi_{\text{MD}}$  models (the latter type evolving as  $\delta\rho/\rho$  in the *linear* regime), which had been the dominant ones for generating backreaction in the old simulations without RNL.

Considering the above results once more in this light, we see that  $\Psi_{\text{Sqr}}$  has indeed performed better than  $\Psi_{\text{Lin}}$  or  $\Psi_{\text{MD}}$ , for example looking much more like best-fit  $\Lambda$ CDM in Figure 4, thus providing better SNIa fits with significantly lower  $\chi_{\text{Fit}}^2$  values (recall Tables 1,2). Furthermore, the output cosmological parameters from the  $\Psi_0$ -optimized  $\Psi_{\text{Sqr}}$  runs (with sufficiently large  $z_{\text{Init}}$  values) were all extremely good, with just the possible exceptions of a slightly low total density (e.g.,  $\Omega_{\text{M}}^{\text{FRW}} \sim 0.94$  for  $z_{\text{Init}} = 25$ ), and a slightly errant CMB angular scale ( $\Delta l_{\text{A}}^{\text{Obs}} \sim 9$ ); but even those discrepancies are quite small given the very simplified nature of these clumping evolution models. (And those discrepancies can be made even smaller with some further development of the models, as will be seen shortly, in Section 3.3).

The only real problem with these  $\Psi_{\text{Sqr}}$  models, and quite an obvious one, is the very high degree of clumping needed in order to generate these results – that is,  $\Psi_{0,\text{Opt}} \simeq 4.1$ . This is right around the extreme upper edge of the ‘reasonable’ range of values for  $\Psi_0$ , which we previously argued should likely lie within  $\Psi_0 \sim 2 - 4$  (and more conservatively, within  $\Psi_0 \sim 2 - 3$ ). Such  $\Psi_{0,\text{Opt}}$  values for  $\Psi_{\text{Sqr}}$  (which are greater than those for  $\Psi_{\text{Lin}}$  or  $\Psi_{\text{MD}}$ ) are large enough as to potentially strain the credibility of causal backreaction as a cosmological solution. As we will see below, however, this concern can be alleviated simply by adding in one important and physically reasonable model parameter as part of these clumping evolution functions: specifically, a parameter representing information about the possible *end* of clumping, as could be triggered in the real universe by galactic feedback.

### 3.3. Early-Saturation Clustering Models: Parameter Flexibility and Paradigm Falsifiability

As our clumping evolution models have so far been defined, each takes on its ‘ultimate’ value,  $\Psi_0$ , at  $t_0$ ; and this may make physical sense in a universe where the effective clumpiness is still growing, so that the value  $\Psi(t_0)$  is not particularly special, but just represents a ‘snapshot’ of  $\Psi(t)$  taken at our particular observation time. But if there is instead some halt to the growth of clumping – due either to the limiting value of  $\Psi(t) \rightarrow 1$  for our pre-RNL simulations, or due to various feedback effects in these new models (which no longer possess a pre-determined upper bound on  $\Psi(t)$ ) – then from a Copernican view, there is nothing necessarily special about the current cosmic epoch, and so there is no reason to assume that the asymptotic value of  $\Psi(t)$  (if there is one) should occur specifically at the present time.

Having already re-evaluated our formalism by interpreting the implementation of  $\Psi_0 > 1$  as representing multiple levels of structure on different cosmic scales, it has become possible for  $\Psi(t)$  to continue increasing without any hard theoretical limit for  $t > t_0$ , perhaps considerably beyond the effective degree of clumping that exists today. On the other hand, if there *does* happen to be some naturally-occurring, effective limit of clumping, then there is no reason to believe that the processes in charge of cosmic clustering would wait until  $t \rightarrow t_0$  to reach it.

As noted above, Cen & Ostriker (2006) show that the nonlinear collapse of material and feedback from star formation have likely acted to shock-heat cosmic baryons to millions of degrees, thus inhibiting clumping – the baryonic part of it, at the very least – by keeping and/or sending a significant portion of the baryons into the superheated IGM; their Figure 1 shows simulation results depicting the rapid increase of very hot baryons in the IGM beginning strongly as of  $z^{\text{Obs}} \sim 3$ .

Additionally, the backreaction effect itself may be helping to put the brakes on structure formation at late times; particularly given the fact that it is generated most strongly within the vicinity of the virializing masses themselves, in high-density regions. In that case, signs of a cosmologically recent slow-down in the growth of clustering (e.g., Vikhlinin et al. 2009) – findings which are viewed as strong evidence in favor of Dark Energy – may instead be indicating the effects of causal backreaction. (Conceivably, feedback from backreaction may also be a contributor to other poorly understood cosmological effects such as galaxy downsizing (Cowie et al. 1996), the cuspy CDM halo problem, and the possible dearth of dwarf satellite galaxies (e.g., Primack 2003).)

What all of this implies is that our clumping evolution functions, as they have been defined in Equations 14a-c, would likely not remain meaningful all the way to  $t \rightarrow t_0$ ; and

thus it is useful to consider how the functional form of our models,  $\Psi(t)$ , might be altered to account in some manner for this effect, to represent the possible late-time softening of the growth of clustering due to astrophysical and/or backreaction-related feedback processes.

The most straightforward way to model this behavior is by implementing an early “saturation time”,  $t_{\text{Sat}} < t_0$  (with  $z_{\text{Sat}} = [(t_0/t_{\text{Sat}})^{2/3} - 1]$ ), representing the time *before* the present epoch at which point the growth of clustering became saturated to a final, fixed value,  $\Psi(t_{\text{Sat}}) \equiv \Psi_0$ . This new clumping evolution function then fixes  $\Psi(t)$  to remain equal to  $\Psi_0$  all the way from  $t_{\text{Sat}}$  to  $t_0$ . Recalling from Section 3.2 that the  $\Psi_{\text{MD}}$  and  $\Psi_{\text{Lin}}$  models only obtain their best fits – and their most ‘concordant’ cosmological parameters – for very late  $t_{\text{Init}}$  values (i.e.,  $z_{\text{Init}} \sim 1.5 - 3$ ), it then makes little sense to outfit those models with an even later  $t_{\text{Sat}} > t_{\text{Init}}$ ; we therefore make this modification only for the  $\Psi_{\text{Sqr}}$  model, which was optimized for concordance with much earlier  $t_{\text{Init}}$  values. The resulting, retrofitted  $\Psi_{\text{Sqr}}$  function for early saturation is thus defined as:

$$\Psi_{\text{Sat}}(t) \equiv \begin{cases} 0 & \text{for } t \leq t_{\text{Init}} , \\ \Psi_0 \left( \frac{t-t_{\text{Init}}}{t_{\text{Sat}}-t_{\text{Init}}} \right)^2 & \text{for } t_{\text{Init}} < t < t_{\text{Sat}} , \\ \Psi_0 & \text{for } t \geq t_{\text{Sat}} . \end{cases} \quad (21)$$

This is obviously a very elementary way of accounting for how astrophysical feedback acts to slow down the growth of clustering (with the resultant lessening of its causal backreaction); but even such an oversimplified model will provide us with valuable cosmological lessons.

As a first run to explore the implications of early saturation, we consider again our earlier, cosmologically successful run with  $\Psi_{\text{Sqr}}$  (functionally identical to  $\Psi_{\text{Sat}}$  with  $z_{\text{Sat}} = 0$ ), which had used  $z_{\text{Init}} = 25$  and its corresponding  $\Psi_{0,\text{Opt}} = 4.1$ ; these results are now compared to those from a new  $\Psi_{\text{Sat}}$  run still using  $z_{\text{Init}} = 25$  and (the now non-optimal)  $\Psi_0 = 4.1$ , but with  $z_{\text{Sat}} = 3$  now imposed – a conservatively early value suggested by the onset of substantial hot baryon injection into the IGM.

The resulting residual Hubble diagrams for the two cases are compared in Figure 5, where the powerful impact of moving from  $z_{\text{Sat}} = 0$  to  $z_{\text{Sat}} = 3$  upon the time-dependence of the observed backreaction can clearly be seen. Not unexpected is the strongly-amplified apparent acceleration effect at early times ( $z^{\text{Obs}} \sim 10$ ), due to the greatly compressed timescale over which clustering grows from  $\Psi(t) = 0$  to  $\Psi(t) = \Psi_0 = 4.1$ . But what may be surprising is how dramatically the effects of these early-developing inhomogeneities become virtually irrelevant at late times, with the effective ‘acceleration’ almost completely fading out by  $z^{\text{Obs}} \sim 1 - 2$ , and the residual Hubble diagram relapsing to a nearly perfect SCDM (i.e., decelerating) cosmology not long after  $z^{\text{Obs}} \sim 1$ .

This is in sharp contrast to what would be expected from the results explored in BBI,

where early-developing clumping provided the strongest ongoing causal backreaction effects due to the ever-growing “inhomogeneity horizons” of observers. The fact that this is no longer the case is clearly due to RNL, which damps such ongoing backreaction effects by slowing down the causal propagation of inhomogeneity information (as well as by diluting the perturbation effects of already-seen inhomogeneities via the extra volumetric expansion), thus greatly restricting the cosmological horizon out from which developing perturbations can affect the observer. As can be inferred from Equations 10,17 above,  $dr/dt \propto \sqrt{1 - I^{\text{RNL}}(t)}$  for inhomogeneity information propagating towards an observer at null-ray speed; and so models with very strong early clumping – particularly those with a very early  $z_{\text{Sat}}$  – drive up the value of  $I^{\text{RNL}}(t)$  so close to unity, so early on, that the propagation of inhomogeneity information is practically frozen to a halt at later times. The cessation of new inhomogeneity information reaching the observer leads to a corresponding freeze in the continued evolution of  $I^{\text{RNL}}(t)$ ; and as is obvious from our metric given by Equation 7, a constant  $I^{\text{RNL}}$  value can simply be transformed away via redefinitions of  $t$  and  $\vec{r}$ , thus making a cosmology with static  $I(t) = I^{\text{RNL}}$  look exactly like a decelerating, matter-dominated SCDM universe. (Interestingly, a considerably stronger late-time acceleration effect can be generated by using a *smaller* value of  $\Psi_0$  for these very early  $z_{\text{Sat}}$  runs, which lessens this ‘freezing’ effect. The best possible SNIa fit for this  $z_{\text{Sat}} = 3$  case is therefore achieved with the relatively low value of  $\Psi_{0,\text{Opt}} = 1.2$ ; though even that remains a very poor fit in absolute terms.)

The importance of such behavior is that it limits the degree to which causal backreaction with RNL can be ‘self-powered’ via the ever-expanding reach of observational horizons, in defiance of a static final  $\Psi_0$  value; a result which increases its dependence upon being ‘driven’ by a continually-growing  $\Psi(t)$  function. As Figure 5 has shown, an early saturation of clumping can lead to a virtually complete shutdown of apparent acceleration not much later. (Though noting again the caveat that nonlinear gravitational effects are not accounted for in any of our models – and that they may indeed be important here, since all of the very-early saturation models with  $z_{\text{Sat}} = 3$  which we tested do have excessively large  $I_0$  values, all significantly exceeding 0.7, with some nearly approaching unity.) These considerations will have important implications for the eventual fate of the universe, as will be discussed below in Section 3.4; but first, we consider their ramifications regarding the *past* cosmic ‘acceleration’ that has already been observed via the supernova data sets.

Since a value of  $z_{\text{Sat}} = 3$  effectively terminates the impact of causal backreaction far too prematurely for it to account for the apparent acceleration seen in the SNIa data from around  $z^{\text{Obs}} \sim 1$  to now, we consider runs with  $z_{\text{Sat}}$  values that are similar to or smaller (i.e., later) than this epoch of acceleration. Specifically, we choose values of  $z_{\text{Sat}} \equiv z_{\text{Sat}}^{\text{FRW}} = (1.0, 0.5, 0.25)$  for study – i.e.,  $t_{\text{Sat}}^{\text{FRW}} \simeq (0.35, 0.5, 0.7)$  – representing times by which the mass fraction of cosmic baryons possessing temperatures of  $T > 10^5\text{K}$  has increased to reach



$\sim 0.4 - 0.5$  (Cen & Ostriker 2006, Figure 1b). These values of  $z_{\text{Sat}}$  are also well-placed to further illuminate the results of Vikhlinin et al. (2009), which demonstrated the significant alteration in clustering behavior (due either to Dark Energy or to causal backreaction) between one cluster sample with  $z > 0.35$  (and particularly its most distant subsample with  $z > 0.55$ ), versus their more nearby cluster sample at  $z < 0.25$ .

Re-optimizing  $\Psi_0$  for each of these chosen  $z_{\text{Sat}}$  values (with  $z_{\text{Init}} = 25$  fixed for all of these runs), the resulting ‘best runs’ with early saturation are those with the parameters:  $(z_{\text{Sat}}, \Psi_0) = (0.25, 2.6)$ ,  $(z_{\text{Sat}}, \Psi_0) = (0.5, 2.3)$ , and  $(z_{\text{Sat}}, \Psi_0) = (1.0, 2.2)$ ; we compare this to the best-fitting  $z_{\text{Sat}} = 0$  run, which had  $\Psi_{0,\text{Opt}} = 4.1$ .

Residual Hubble curves for these four runs are plotted in Figure 6, where we see that while these early-saturation runs are no longer effectively indistinguishable from best-fit  $\Lambda$ CDM (as was the  $z_{\text{Sat}} = 0$  run), they are nevertheless very close to it – particularly within the redshift range containing most of the SNIa – thus providing quite good fits to these data.

The complete fit quality results and cosmological output parameters for these runs are presented in Table 3. First, we note that there are limits to the largest value of  $z_{\text{Sat}}$  which may practically be used, since we see that as  $z_{\text{Sat}}$  gets as high as 1.0, the fit probability  $P_{\text{Fit}}$  gets progressively worse (i.e.,  $\chi_{\text{Fit}}^2$  begins to grow unacceptably large), the cosmological parameters become increasingly ‘discordant’ (particularly  $\Omega_{\text{M}}^{\text{FRW}}$  and  $l_{\text{A}}^{\text{Obs}}$ ), and there are even concerns that the formalism itself begins to break down due to gravitationally nonlinear effects, given the disturbingly large value of  $I_0$ .

If we restrict ourselves to  $z_{\text{Sat}} \lesssim 0.5$ , however, then at a cost of only a small increase in  $\chi_{\text{Fit}}^2$ , the situation gets considerably better with the use of nonzero  $z_{\text{Sat}}$  in several crucial ways. Considering the  $z_{\text{Sat}} = 0.25$  case in particular, moving away from  $z_{\text{Sat}} = 0$  has improved the match to the CMB data and the verification of spatial flatness (better  $l_{\text{A}}^{\text{Obs}}$  and  $\Omega_{\text{M}}^{\text{FRW}}$  values, respectively), while remaining essentially as good in terms of the other cosmological parameters, with just a tiny degradation in the fit probability (by  $\Delta P_{\text{Fit}} = -0.025$ ). But most importantly, we see that all of this been achieved with a *much* lower  $\Psi_0$  value – Table 3 showing how  $\Psi_{0,\text{Opt}}$  decreases with increasing  $z_{\text{Sat}}$ , in general – dropping all the way from  $\Psi_{0,\text{Opt}} = 4.1$  for  $z_{\text{Sat}} = 0$ , to  $\Psi_{0,\text{Opt}} = 2.6$  for  $z_{\text{Sat}} = 0.25$ . This is now well within the  $\Psi_0 \sim 2 - 3$  range of ‘reasonable’ values for hierarchical clustering, as was specified earlier in Section 3.2.

(In addition, we have also conducted fits to a more recent supernova data set, the SCP Union2 SNIa compilation (Amanullah et al. 2010); and when we minimize  $\chi_{\text{Fit}}^2$  for the  $z_{\text{Sat}} = 0.25$  case with respect to the Union2 data, rather than the Union1 data, we still get similar results: an excellent fit with  $\chi_{\text{Fit}}^2 = 543.6$  (compared to  $\chi_{\text{Fit}}^2 = 542.7$  for  $\Lambda$ CDM)

and  $P_{\text{Fit}} \simeq 0.6$ ; only a slightly higher clumping strength value of  $\Psi_{0,\text{Opt}} = 2.8$ ; and similar cosmological parameters that are also quite acceptable. Only the unperturbed matter density is slightly high with  $\Omega_{\text{M}}^{\text{FRW}} = 1.13$ ; but as discussed above, this may be due to the adopted value of  $\Omega_{\text{M}}^{\text{Obs}} \equiv 0.27$  being slightly too large.)

In consequence, it is justified to say that we have in every sense re-obtained a successful alternative concordance with causal backreaction in the presence of recursive nonlinearities, having generated the proper amount (and temporal behavior) of apparent acceleration – as evidenced by a fit to the SNIa data that is very nearly as good as that achievable with best-fit  $\Lambda$ CDM (even *without* performing a rigorous  $\chi_{\text{Fit}}^2$ -minimization search over our model parameter space) – as well as having produced output cosmological parameters that are more than acceptably consistent with a variety of complementary cosmic measurements. The price to be paid to achieve this goal, due to the incorporation of recursive nonlinearities, is the necessity of permitting  $\Psi_0$  values in excess of unity – which though going against the original interpretation of this (heuristic) model parameter, as defined in BBI, does seem justifiable in a realistic cosmology exhibiting hierarchical structure formation on a variety of scales. On the other hand, a new benefit of these results is the shifted focus from  $\Psi_{\text{MD}}$  models to  $\Psi_{\text{Sqr}}$  models, equivalent to a shift in emphasis from linearized matter density perturbations to nonlinear density perturbations; a new emphasis which in fact makes much more sense for a causal backreaction paradigm depending upon vorticity- and velocity-dispersion-generated virialization as the fundamental origin of structure-induced perturbations to the observed cosmological metric.

One last (yet very important) consideration still remains regarding early saturation, though, relating to its impact upon the very late-time behavior of the cosmic evolution. One way to approach this, is to consider *why* the optimized value of  $\Psi_0$  drops so precipitously with increasing  $z_{\text{Sat}}$ , so conveniently solving our problem by reducing  $\Psi_{0,\text{Opt}}$  to believable values. To understand why this happens, consider the clumping evolution functions, themselves, for the early saturation models that we have studied; plots of these  $\Psi(t)$  functions are shown in Figure 7.

From these plotted curves, we see that despite the vast differences in  $\Psi_{0,\text{Opt}}$  for the  $z_{\text{Sat}} = 0$  case versus those with  $z_{\text{Sat}} \neq 0$ , as long as one does not use too large a value of  $z_{\text{Sat}}$  (sticking to, say,  $z_{\text{Sat}} \lesssim 0.5$ ), then the degree of clumping  $\Psi(t)$  at *mid-range* values of  $z$  (e.g.,  $z^{\text{FRW}} \sim 0.2 - 0.5$ ) actually remains fairly similar from run to run. The distinctively huge increase from  $\Psi(t) \sim 2.5$  to  $\Psi(t) \sim 4$  for the  $z_{\text{Sat}} = 0$  case does not actually happen until very late times,  $z^{\text{FRW}} \lesssim 0.2$ . But why should completely different behaviors of  $\Psi(t)$  at late times have such a small effect upon the fits to the SNIa data? The answer is twofold: first, due to a lack of sensitivity of the data to such changes; and second, due to the nature

of causal backreaction, itself.

For the first issue, consider that most of the SNIa included in these supernova compilations for measuring the cosmic acceleration are located at fairly high redshift; it is therefore unsurprising that the evolution of  $\Psi(t)$  *after* the epoch of these supernovae should have little effect upon the acceleration measured by those high- $z$  SNIa, regardless of whether  $\Psi(t)$  experiences a continued increase or a saturation. But, even if lower- $z$  SNIa were also included in the study, and could be trusted to accurately map out the Hubble flow despite their local peculiar motions, there should still be little effect other than a late-time offset, perhaps registered as a small change in  $H_0^{\text{Obs}}$ . As noted by Linder (2007), simple cosmic evolution functions that are relatively insensitive to time variations tend to measure an averaged cosmological equation of state around a ‘pivot’ redshift of about  $z^{\text{Obs}} \approx 0.4$ . And so it is understandable why the detailed behavior of  $\Psi(t)$  after this crucial epoch should end up having little effect upon the precise amount of apparent acceleration measured.

For the second issue, we recall from Equation 5 that the amount of causal backreaction due to a spherical shell at coordinate radius  $r$  will be proportional to  $dM/r \propto r^2/r \propto r$ , and so very late clumping – which corresponds to relatively small look-back times  $t_{\text{ret}}$ , and thus small distances  $r$  – will simply not involve a sufficiently large amount of inhomogeneous mass to generate significant causal backreaction. Thus the detailed dynamics of inhomogeneities at higher  $z$  (and larger  $r$ ) – assuming distances not so far away as to get damped by RNL, or having look-back times so far back relative to  $t_{\text{Init}}$  as to have very small clustering,  $\Psi(t_{\text{ret}})$  – will be more important in determining the detailed effects of causal backreaction than would the very late ( $z \rightarrow 0$ ) behavior of clumping.

The overall result is that there is a parameter degeneracy for causal backreaction models, where one can reduce  $\Psi_0$  in tandem with an increase in  $z_{\text{Sat}}$ , without much change in the quality of the fit to the actual SNIa data. This degeneracy has a beneficial aspect, in that it has allowed us to successfully create an alternative concordance with causal backreaction – and to do so in a flat, matter-only universe without any form of Dark Energy – while using astrophysically realistic values of  $\Psi_0$ . But it has a negative aspect, as well, in that it lessens our ability to predict precise ranges for the late-time cosmological parameters that would be output by the various (successfully concordant) models in this formalism. Measurable cosmological parameters such as  $H_0^{\text{Obs}}$ ,  $w_0^{\text{Obs}}$ , and  $j_0^{\text{Obs}}$  are defined – in theory, at least – in terms of the  $z^{\text{Obs}} \rightarrow 0$  behavior of Taylor expansions of the luminosity distance function,  $d_L(z^{\text{Obs}})$ . Hence, while a variety of  $\Psi(t)$  functions may all provide good fits to the key SNIa located at mid-to-high redshifts, these functions may all have quite different  $t \rightarrow 0$  behaviors, and thus very significant differences in their cosmological output parameters.

In particular, consider again the first three of the four runs in Table 3. As one goes

from  $z_{\text{Sat}} = 0$  to  $z_{\text{Sat}} = 0.5$ , we see that  $H_0^{\text{Obs}}$  decreases below the  $\Lambda\text{CDM}$  Concordance value of  $H_0^{\text{Obs}} \simeq 70$ ; but yet, the difference is small enough to not be a serious concern. For  $w_0^{\text{Obs}}$ , obtained from one more differentiation of  $d_L$ , the difference is larger, going from  $w_0^{\text{Obs}} \sim -0.75$  to  $w_0^{\text{Obs}} \sim -0.59$ ; and yet, the precise numerical value of the cosmic ‘equation of state’  $w_0^{\text{Obs}}$  is of no great concern to us here – since it is not our task to pin down the physics of some hypothesized form of Dark Energy, but merely to reproduce the cosmological observations – so long as a good fit with a sufficient amount of apparent acceleration can be produced, as has indeed been accomplished.

The biggest change, however, occurs for  $j_0^{\text{Obs}}$  – obtained via yet another differentiation of  $d_L$  – which drops all the way from  $j_0^{\text{Obs}} \sim 1.7$  for  $z_{\text{Sat}} = 0$ , down through the  $\Lambda\text{CDM}$  value of  $j_0 \equiv 1$  and far past it, even going negative for  $z_{\text{Sat}}$  values that still provide decent SNIa fits.

A small part of this change may be due to the highly simplified nature of the  $\Psi_{\text{Sat}}$  functions that we use; in particular, since we obtain a Hubble curve through two integrations of  $\Psi(t)$  – that is,  $\Psi(t) \rightarrow I(t)$ , and then  $I(t) \rightarrow d_L$  (cf. Equations 6-11) – the  $j_0^{\text{Obs}}$  parameter (obtained from three differentiations of  $d_L$ ) essentially contains one differentiation of  $\Psi(t)$ . As is obvious from Figure 7, our simple  $\Psi_{\text{Sat}}$  functions are not differentiable at  $z_{\text{Sat}}$ , meaning that  $q^{\text{Obs}}(z)$  (and thus  $w^{\text{Obs}}(z)$ ) will also be non-differentiable there, and so  $j^{\text{Obs}}(z)$  will pick up an actual discontinuity there. Still, the discontinuity is not large enough to account for the huge overall differences in  $j_0^{\text{Obs}}$  for the different  $z_{\text{Sat}}$  values; and most of the effect of the jump in  $j^{\text{Obs}}(z)$  at  $z_{\text{Sat}}$  is almost certainly real, due to the real change in the cosmic evolution at that point, and would likely still take place to a very similar degree (just more spread out in time) for some more complicated  $\Psi_{\text{Sat}}$  functions designed to apply smoothing at  $z_{\text{Sat}}$ . In any case, the set of runs in Table 3 does fairly clearly establish the trend that increasing  $z_{\text{Sat}}$  away from zero leads to a steady decrease in the final value of  $j_0^{\text{Obs}}$ .

What we can conclude with some certainty, unfortunately, is that we have lost any reasonable degree of predictability for this  $j_0^{\text{Obs}}$  parameter in the causal backreaction paradigm, due the weak dependence of the backreaction upon the very-late-time behavior of  $\Psi(t)$ , and the resulting degeneracy in  $(z_{\text{Sat}}, \Psi_0)$ . This is significant, because of the different possible ways suggested in BBI to distinguish between causal backreaction and Cosmological Constant  $\Lambda\text{CDM}$  (or any similar form of Dark Energy), in order to provide our paradigm with a falsifiable test, the clearest signature by far was the search for  $j_0^{\text{Obs}} \gg 1$ . For all intents and purposes, the reliability of this signature now appears to be gone, and some more intricate means will obviously be needed to distinguish causal backreaction from even the simplest,  $\Lambda$ -like version of Dark Energy (though  $j_0^{\text{Obs}} \neq 1$  would still rule out  $\Lambda\text{CDM}$  in favor of *some* alternative model). Thus while the use of early saturation has greatly enhanced the prospects

for achieving an alternative cosmic concordance with realistic values of the clumping parameter  $\Psi_0$ , the incorporation of this additional degree of freedom in the models has made it significantly more challenging to definitively replace the paradigm of Dark Energy with that of causal backreaction, without resorting to aesthetic arguments of a subjective nature.

### 3.4. The New Cosmic Future: How Recursive Nonlinearities Affect the Possibility of Long-Term Acceleration from Causal Backreaction

If appropriate observational tests should eventually be able to demonstrate causal backreaction as superior to Dark Energy as the driver of the cosmic evolution, then one final question of great importance would of course be: What is the ultimate fate of the universe?

This topic was discussed in detail in BBI, in which it was found that the long-term cosmic fate depends upon which way the balance tips between the forces working to power the cosmic ‘acceleration’, versus the opposing factors acting to restrain it. For the former, the only real influence working to keep the apparent acceleration going (and perhaps ultimately promote it in strength to a real volumetric acceleration) was the ever-expanding causal horizon, growing in time, out from which an observer can ‘see’ substantial inhomogeneities – i.e., the farthest distance from the observer out to which  $t_{\text{ret}} > t_{\text{Init}}$ ,  $\Psi(t_{\text{ret}}) \gg 0$  are still true.

For opposition to the acceleration, one source of restraint is the FRW expansion of the universe itself, which exerts a natural damping effect upon causal backreaction by diluting the density of inhomogeneities, simply by pulling them farther away from one another (and from any given cosmological observer) over time. Also acting to limit a possible long-term acceleration was the inevitable saturation presumed for  $\Psi(t)$ , which – in our original interpretation of this measure of clumping, as described in BBI – would be limited by an upper bound of  $\Psi \rightarrow 1$ .

Considering all of these factors, analytical approximations were derived for the (pre-RNL) metric perturbation function  $I(t)$  as  $t \rightarrow \infty$ ; and it was found that  $I(t)$  always asymptotes to a constant numerical value for  $\Psi(t)$  functions evolving as a simple power of  $t$ ,  $\Psi(t) \propto t^N$ . This asymptotic value of  $I(t)$  is larger for smaller  $N$ , with it being equal to unity (implying a complete breakdown of the Newtonian-perturbed metric) for  $N = 2/3$  (i.e.,  $\Psi = \Psi_{\text{MD}}$ ). Thus a fully general-relativistic acceleration at late times due to causal backreaction did appear to be realistically possible, according to the formalism of BBI – though of course that conclusion was made pending the still-undetermined effects of recursive nonlinearities, and other complications.

In this paper, however, we will have to revise our expectations, since the incorporation of RNL (recursive nonlinearities) has made the prospects of an ‘eternal’, self-powered acceleration seem far less likely. We can conclude this despite the fact that  $I(t)$  is no longer necessarily amenable to a simple analytical analysis, even for  $t \rightarrow \infty$ . One point in favor of such a conclusion is that RNL has forced us to change to  $\Psi(t) \propto t^N$  functions with larger exponents  $N$  in order to re-establish a concordance – i.e., moving from  $\Psi_{\text{MD}}$  and  $\Psi_{\text{Lin}}$  before, to  $\Psi_{\text{Sqr}}$  now – and as our previous results have shown, larger exponents in  $\Psi(t)$  lead to smaller late-time values of  $I(t)$  (even if we no longer know its exact asymptotic behavior), thus implying a less general-relativistic, less ‘accelerative’ long-term evolution. But an even more important factor is what we learned about the impact of the ultimate ‘saturation’ of the clumping evolution function  $\Psi(t)$  at some final, fixed numerical value, as was depicted in Figure 5. This result (and other simulation runs that we have done along these lines) clearly demonstrate that RNL, which acts to stall the expansion of an observer’s “inhomogeneity horizon” – particularly so in cosmologies with strong early-time backreaction – will largely ‘shut off’ all apparent acceleration effects not long after the ongoing clustering and virialization have ceased, once  $\Psi(t)$  has settled down to some mostly-constant final value. This behavior certainly works against the possibility of an ‘eternally’ (or even long-term) ‘accelerating’ universe.

The one enhancement introduced in this paper which might possibly help lead to a long-term acceleration, is the now fundamentally unbounded nature of  $\Psi(t)$  due to hierarchical clustering (assuming that an effective end to clustering is not imposed explicitly by early saturation, as we did in fact choose to impose for our models in Section 3.3). But while this change in interpretation allowing  $\Psi(t) > 1$  is indeed based upon real physics, is it strong enough to keep the ‘acceleration’ going continually, deep into the future? The answer to this question is naturally uncertain: on (relatively) small scales, clustering has never ceased, as star clusters and small galaxies continue to merge (with new virialization) into large galaxies; galaxies continue to merge into galactic clusters; and so on. Yet, one would realistically expect to find steadily diminishing returns on such ‘small’ scales. Any real hope for a continuing acceleration would seem to rest upon the future clustering behavior on extraordinarily *large* scales – a realm of structure formation with no real upper limit, as superclusters eventually manage to self-virialize internally, then begin themselves to merge into even larger structures, and so on, ad infinitum. Higher and higher scales of clustering take exponentially longer to complete than the levels below them, though, and it is not clear how large the effective ‘inhomogeneity horizon’ for causal backreaction can ever practically become – especially given the fact that the cosmic acceleration itself tends to impede the expansion of observational horizons. A truly long-term cosmic acceleration (apparent or real) into the far future would therefore seem very difficult to accomplish using

causal backreaction with recursive nonlinearities; though such conclusions cannot be considered definitive without more detailed cosmological simulations, employing a significantly more sophisticated treatment of the effects of vorticity and virialization than we have used in these calculations so far, given our toy models for  $\Psi(t)$ , and therefore  $I(t)$ .

There are still two remaining wildcards, however, which were discussed in BBI and must be mentioned again here. The first one is the possible advent of truly general-relativistic perturbations, causing the breakdown of our Newtonian-perturbed metric approximation (Equation 2), and the failure of our treatment of the individual perturbations due to the multitude of locally-clumped masses as being linearly summable. The possibility of such a complication still exists, as is made obvious (for example) by the very large  $I_0$  values that we typically find for early-saturation runs with large  $z_{\text{Sat}}$  settings (e.g., the  $z_{\text{Sat}} = 1$  case from Table 3). As noted above in Section 3.3, the fact that the propagation of inhomogeneity information obeys the proportionality  $dr/dt \propto \sqrt{1 - I^{\text{RNL}}(t)}$ , means that the flow of such information will be choked off whenever  $I^{\text{RNL}}$  approaches unity, thus freezing the expansion of the relevant inhomogeneity horizons, thereby locking  $I^{\text{RNL}}(t)$  nearly in place at whatever actual value that it has managed to grow to by that time. (This is in fact the biggest reason why the  $z_{\text{Sat}} = 3$  model from Figure 5 experienced such an abrupt shut-off of its apparent acceleration so quickly after the growth of its clumping evolution function  $\Psi(t)$  had ceased.) What we cannot know from our formalism, however, is how to physically interpret the effects of a metric perturbation function  $I^{\text{RNL}}(t)$  that is hovering around a nearly fixed value, but where that value is always slowly asymptoting towards unity. Does it look almost exactly like a decelerating  $\Lambda$ CDM universe, since a constant  $I^{\text{RNL}}(t)$  can simply be transformed away through coordinate redefinitions? Or would it instead be a universe perpetually appearing to be right on the verge of undergoing a runaway acceleration, just never quite doing it, basically ‘riding the edge’ forever? (Perhaps succeeding, at least, at producing a hesitating, stop-and-go accelerating behavior.) Or on the other hand, does the proximity of  $I^{\text{RNL}}(t)$  to unity manage to override all other considerations, and lead to an actual, volumetric, runaway acceleration? The real answers to these questions cannot be determined without at least some nonlinear gravitational terms being added into the formalism, if not actually requiring a fully general-relativistic treatment. But while the quantitative calculation of such effects to determine their physical implications is beyond the scope of the causal backreaction formalism that has been presented here (or in BBI), it is clear that the sum of innumerably many Newtonian-level perturbations is indeed capable of driving the total cosmological metric perturbation right up to the breaking point, where a ‘real’ cosmic acceleration (by any definition) may very possibly take over, and for an indeterminate period of time.

Last of all considerations, though, is the one that can least safely be neglected: and

that is the eventual breakdown of our smoothly-inhomogeneous approximation, as increasing clumpiness leads to fundamentally non-negligible anisotropies across much of the observable universe itself (e.g., the “Dark Flow” of Kashlinsky et al. 2010); a scenario which in BBI was termed the “Big Mess”. This final, virtually certain breakdown of the Cosmological Principle is the ultimate game-changer, and questions about the possibility of a ‘permanent’ cosmic acceleration due to causal backreaction then become just as hard to define as they are to answer, as the fundamental FRW basis of cosmological analysis finally breaks down entirely.

#### 4. SUMMARY AND CONCLUSIONS

In this paper, we have revisited the causal backreaction paradigm introduced in Bochner (2011), for which the apparent cosmic acceleration is generated not by any form of Dark Energy, but by the causal flow of information coming in towards a typical cosmological observer from a multitude of Newtonian-strength perturbations, each one due to a locally clumped, virializing system. Self-stabilized by vorticity and/or velocity dispersion, such perturbations are capable of generating positive volume expansion despite their individually-Newtonian natures. Noting that previous ‘no-go’ arguments against Newtonian-level backreaction are based upon non-causal backreaction frameworks, we see that the sum total of these small but innumerable perturbations adds up to an overall effect that is strong enough to explain the apparent acceleration as detected by Type Ia supernovae, as well as permitting the formulation of an alternative cosmic concordance for a matter-only, spatially-flat universe.

Our purpose here has been to develop and test a second-generation version of this causal backreaction formalism, filling in one of the most important gaps of the original ‘toy model’ by including what we have termed “recursive nonlinearities” – specifically referring to the process by which old metric perturbation information tends to slow down the causal propagation of all future inhomogeneity information, therefore reducing the effective cosmological range of causal backreaction effects, and thus damping the strength of their overall impact upon the cosmic evolution and upon important cosmological observations.

Utilizing the new simulation program introduced here, which now incorporates recursive nonlinearities into causal backreaction, we find profound differences in the resulting cosmological model calculations. For a given magnitude of self-stabilized clustering assumed for large-scale structure, denoted by dimensionless model input parameter  $\Psi_0$ , the overall power of causal backreaction is now considerably weaker, in addition to fading out relatively rapidly after the growth of clustering ceases. This is unlike the results of the original model, in which causal backreaction effects would continue to grow regardless of any late-time saturation of



clustering, due to the causally-expanding “inhomogeneity horizon” seen by an observer which continually brings more ‘old’ inhomogeneities into view from ever-greater cosmic distances.

After discussion of some of the possible reasons for which causal backreaction may now appear to fall short of its cosmological goals – either due to issues regarding the fundamental mechanism itself, or due to our highly simplified treatment of it – we then considered a very straightforward way in which the paradigm may be fully recovered as a cosmological replacement for Dark Energy: all that is needed is the adoption of  $\Psi_0$  values greater than unity. Though representing an ad-hoc modification of the original formalism, the change makes astrophysical sense in a number of ways. Rather than viewing the clumping evolution function  $\Psi(t)$  as simply representing the fraction of cosmic matter in the ‘clumped’ versus ‘unclumped’ state at any given time,  $\Psi(t)$  can now be recognized (more realistically) as representing the total backreaction effect of hierarchical structure formation in the universe, where clustering and virialization take place simultaneously on a number of different cosmic length scales – from stellar clusters, to individual galaxies, to galaxy clusters, etc. Model input parameter  $\Psi_0 \equiv \Psi(t_0)$  is now interpreted as the effective number of ‘levels’ of completed clustering that exists (at current time  $t_0$ ) in the large-scale structure when one sums over the (partial or total) clustering of matter on all relevant cosmic scales.

Given this enlarged parameter space with  $\Psi_0 > 1$  now permitted, we once again find a selection of model cosmologies that succeed (despite the damping effects of recursive nonlinearities) at reproducing the observed cosmic acceleration, while also re-establishing an alternative cosmic concordance by producing output parameters that match the observables derived from several of the most important cosmological data sets. Furthermore, astrophysical considerations regarding the necessary *input* parameters for these apparently successful models – specifically, the need to assume a sufficiently early beginning of clustering – results in a preference by the new formalism for  $\Psi(t)$  models that reflect the late, nonlinear phase of structure formation. This is an improvement over the old formalism without recursive nonlinearities – which had preferred models that embody the early phase of clustering, with linearized matter fluctuations – since it is this final, nonlinear stage of clustering during which virialization occurs via the generation of vorticity and velocity dispersion, and hence represents the more astrophysically reasonable source of substantial causal backreaction.

Noting that the only problem still remaining for this new concordance is the somewhat excessively large amount of clustering required to achieve it – that is,  $\Psi_0 \simeq 4$ , rather than what we consider to be more reasonable values like  $\Psi_0 \sim 2 - 3$  – we then determined that this problem could be successfully fixed (i.e., a good concordance generated with  $\Psi_0 < 3$ ) by introducing “early saturation”, in which the clumping evolution function  $\Psi(t)$  reaches its ultimate value of  $\Psi_0$  somewhat in the past ( $z \sim 0.25$ ), and then changes little thereafter. This

is a highly reasonable adjustment to the formalism, since in the real universe “gastrophysics” feedback exists which creates superheated baryons, sending large amounts of material back into the intergalactic medium, thereby slowing down the continued clustering of matter at late times; not to mention the likely slowdown of clustering due to the feedback effects of the backreaction, itself.

The only major drawback of this new feature is the addition of an extra model input parameter – the epoch of saturation,  $z_{\text{Sat}}$  – which results in a degeneracy within  $(z_{\text{Sat}}, \Psi_0)$ -space, providing a range of models that all fit the Type Ia supernova data well, yet lead to significant differences for certain output cosmological parameters. The greatest variation in the output results due to this degeneracy occurs for the observable jerk parameter,  $j_0^{\text{Obs}}$ , hence implying a loss of predictability for  $j_0^{\text{Obs}}$  by our causal backreaction formalism. This is a significant loss, given the previous findings from Bochner (2011) (without recursive nonlinearities) which had indicated that  $j_0^{\text{Obs}} \gg 1$  was the most distinctive signature of causal backreaction, thus serving as the clearest way for distinguishing it from Cosmological Constant  $\Lambda$ CDM (or from anything close to it), since flat  $\Lambda$ CDM always requires  $j_0 = 1$ . It thus becomes more difficult to find a falsifiable test of the causal backreaction paradigm, a test that is needed to definitively distinguish it from Dark Energy in order to eventually rule out one cosmological approach in favor of the other.

Finally, concerning the ‘ultimate’ fate of the universe, we note that the incorporation of recursive nonlinearities tends to shut down any strong apparent acceleration effects fairly quickly once the ongoing clustering (i.e., the continued growth of  $\Psi(t)$ ) finally stops. Even more dramatic is the way in which the metric perturbation function,  $I^{\text{RNL}}(t)$ , becomes essentially locked in place when approaching too close to unity, making it an even greater obstacle in terms of preventing the acceleration (apparent or otherwise) from completely taking over the cosmic evolution. This makes the scenario of a perpetual, ‘eternal’ acceleration seem even less likely than it already did in Bochner (2011); though the now-unbounded nature of  $\Psi(t)$  could potentially provide some aid in producing a long-term acceleration, as long as virialized structure can continue to form on ever-larger cosmic scales, without any fundamental upper limit to the sizes of coherent structures. Furthermore, the question of the ultimate cosmic fate is once again complicated by the possible backreaction contributions of gravitationally nonlinear terms, and the (unavoidable) eventual breakdown of the approximation of the universe as “smoothly-inhomogeneous” – both complications representing scenarios which our toy-model formalism is not presently designed to account for.

In summary, we conclude that our causal backreaction formalism remains successful at generating an alternative cosmic concordance for a matter-only universe, without requiring any form of Dark Energy; though the necessary incorporation of recursive nonlinearities into

these models implies that a significantly stronger amount of such backreaction than before is now needed, acting throughout the crucial ‘acceleration epoch’ of  $z \sim 0.2 - 2$  or so, in order to provide a degree of observed acceleration sufficient to match the cosmological standard candle observations.

I am grateful to William Chan for computational support.

## REFERENCES

- Amanullah, R., et al. 2010, ApJ 716, 712; preprint (arXiv:1004.1711v1)
- Arkani-Hamed, N., Hall, L. J., Kolda, C., & Murayama, H. 2000, Phys. Rev. Lett. 85, 4434; preprint (arXiv:astro-ph/0005111v2)
- Biswas, T., Mansouri, R., & Notari, A. 2007, J. Cosmology Astropart. Phys. 0712, 017; preprint (arXiv:astro-ph/0606703v2)
- Bochner, B. 2011, preprint (arXiv:1109.4686v3); A briefer overview version is available as: 2011, preprint (arXiv:1109.5155v3)
- Buchert, T., & Ehlers, J. 1997, A&A 320, 1; preprint (arXiv:astro-ph/9510056v3)
- Buchert, T., Kerscher, M., & Sicka, C. 2000, Phys. Rev. D62, 043525; preprint (arXiv:astro-ph/9912347v2)
- Caldwell, R. R., Dave, R., & Steinhardt, P. J. 1998, Phys. Rev. Lett. 80, 1582; preprint (arXiv:astro-ph/9708069v2)
- Cattoën, C., & Visser, M. 2008, Phys. Rev. D78, 063501; preprint (arXiv:0809.0537v1)
- Cen, R., & Ostriker, J. P. 2006, ApJ 650, 560; preprint (arXiv:astro-ph/0601008v1)
- Cowie, L. L., Songaila, A., Hu, E. M., & Cohen, J. G. 1996, AJ 112, 839; preprint (arXiv:astro-ph/9606079v1)
- Franklin, J., & Baker, P. T. 2007, Am. J. Phys. 75, 336
- Hawking, S. W., & Ellis, G. F. R. 1973, The large scale structure of space-time (Cambridge, UK: Cambridge University Press)
- Hu, W. 1998, ApJ 506, 485; preprint (arXiv:astro-ph/9801234v2)

- Kaloper, N., Kleban, M., & Martin, D. 2010, Phys. Rev. D81, 104044; preprint (arXiv:1003.4777v3)
- Kantowski, R. 2003, Phys. Rev. D68, 123516; preprint (arXiv:astro-ph/0308419v1)
- Kashlinsky, A., Atrio-Barandela, F., Ebeling, H., A. Edge, & Kocevski, D. 2010, ApJ 712, L81; preprint (arXiv:0910.4958v3)
- Kerr, R. P. 1963, Phys. Rev. Lett. 11, 237
- Kolb, E. W., & Turner, M. S. 1990, The Early Universe (Redwood City, CA: Addison-Wesley)
- Komatsu, E., et al. 2011, ApJS 192, 18; preprint (arXiv:1001.4538v3)
- Kowalski, M., et al. 2008, ApJ 686, 749; preprint (arXiv:0804.4142v1)
- Linder, E. V. 2007, preprint (arXiv:0708.0024v1)
- McVittie, G. C. 1933, MNRAS 93, 325
- Perlmutter, S., et al. 1999, ApJ 517, 565; preprint (arXiv:astro-ph/9812133v1)
- Primack, J. R. 2003, preprint (arXiv:astro-ph/0312549v1)
- Riess, A. G., et al. 1998, AJ 116, 1009; preprint (arXiv:astro-ph/9805201v1)
- Schwarz, D. J. 2010, preprint (arXiv:1003.3026v1)
- Springel, V., et al. 2005, Nature 435, 629; preprint (arXiv:astro-ph/0504097v2)
- Tomita, K. 2001, Prog. Theor. Phys. 106, 929; preprint (arXiv:astro-ph/0104141v5)
- Trodden, M. 2008, Int. J. Mod. Phys. D16, 2065; preprint (arXiv:astro-ph/0607510v1)
- Turner, M. S. 2002a, ApJ 576, L101; preprint (arXiv:astro-ph/0106035v2)
- Turner, M. S. 2002b, Int. J. Mod. Phys. A17S1, 180; preprint (arXiv:astro-ph/0202008v1)
- Vikhlinin, A., et al. 2009, ApJ 692, 1060; preprint (arXiv:0812.2720v1)
- Weinberg, S. 1972, Gravitation and Cosmology (New York, NY: John Wiley & Sons, Inc.)

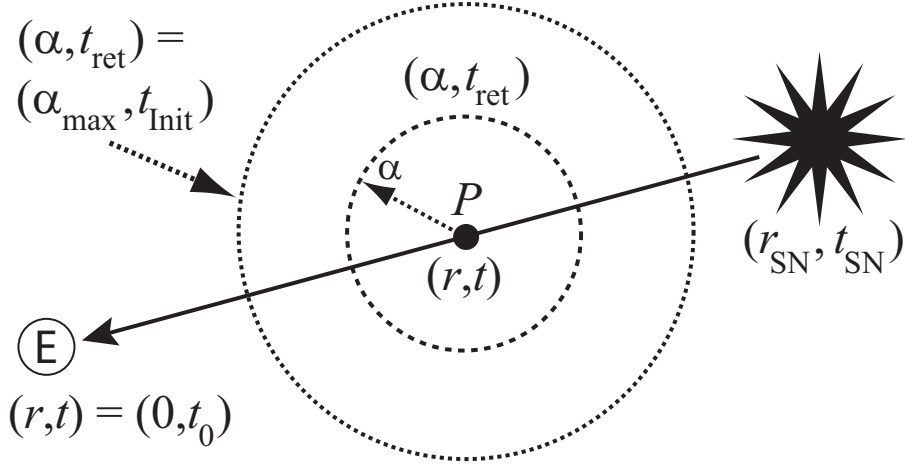


Fig. 1.— Geometry for computing the inhomogeneity-perturbed metric at each point along the integrated path of a light ray from a supernova to our observation point at Earth.

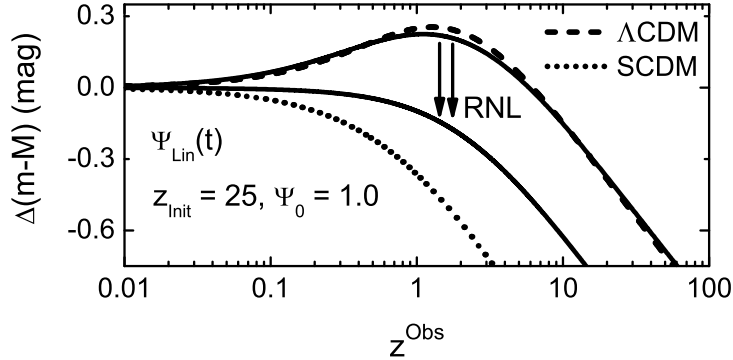


Fig. 2.— Residual Hubble diagrams for the causal backreaction model  $\Psi_{\text{Lin}}(t)$  with  $(z_{\text{Init}}, \Psi_0) = (25, 1.0)$ , where the upper solid line represents the old version of the simulated cosmology without recursive nonlinearities (RNL), and the lower solid line represents the new version with RNL. Shown along with them for comparison (broken lines) are the flat SCDM and (Union1-best-fit,  $\Omega_\Lambda = 0.713$ ) Concordance  $\Lambda$ CDM cosmologies.

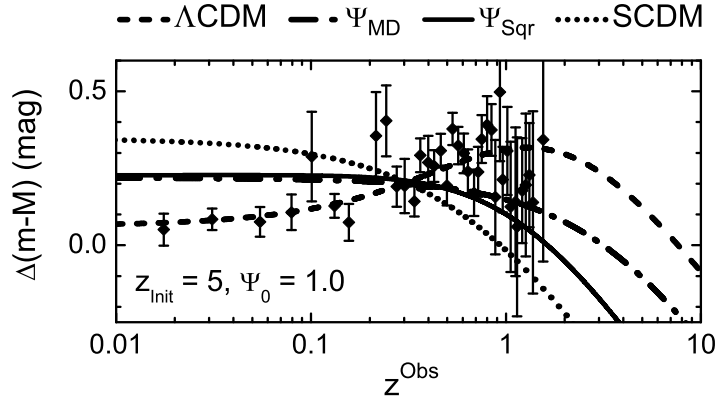


Fig. 3.— Residual Hubble diagrams for the two ‘best’  $\Psi_0 \leq 1$  runs (as described in the text), selected from the new simulations with RNL but with the choice of model input parameters restricted to those used in BBI; specifically, these  $\Psi_{\text{MD}}$  and  $\Psi_{\text{Sqr}}$  curves both have  $(z_{\text{Init}}, \Psi_0) = (5, 1.0)$ . Also plotted here are the Union1-best-fit flat SCDM and Concordance  $\Lambda\text{CDM}$  ( $\Omega_\Lambda = 0.713$ ) cosmologies. Shown along with these curves are the SCP Union1 SNIa data, here binned and averaged for visual clarity (bin size  $\Delta\text{Log}_{10}[1+z] = 0.01$ ). Each theoretical model is individually optimized in  $H_0^{\text{Obs}}$  to minimize its  $\chi_{\text{Fit}}^2$  with respect to the Union1 SNIa data set; and for simplicity, instead of moving the SNIa data up or down for each different optimized  $H_0^{\text{Obs}}$  value, the optimization is depicted here by plotting the residual Hubble diagram of the SNIa data versus a coasting universe of a single, fixed Hubble constant ( $H_0^{\text{Obs}} = 72 \text{ km s}^{-1}\text{Mpc}^{-1}$ ), and then displacing each theoretical curve vertically, relative to the SNIa data, as appropriate for each fit.

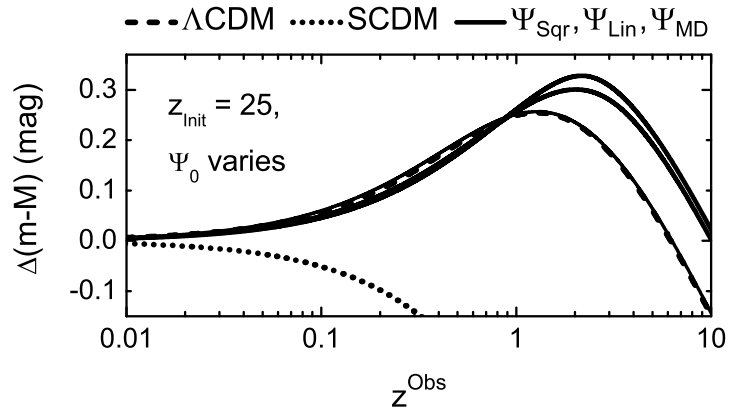


Fig. 4.— Residual Hubble diagrams for three of the ‘best’ runs with  $\Psi_0 > 1$  (as described in the text), using model input parameters (solid lines increasing from lowest to highest):  $\Psi_{\text{Sqr}}$  with  $(z_{\text{Init}}, \Psi_0) = (25, 4.1)$  (curve almost indistinguishable from  $\Lambda$ CDM);  $\Psi_{\text{Lin}}$  with  $(z_{\text{Init}}, \Psi_0) = (3, 3.3)$ ; and  $\Psi_{\text{MD}}$  with  $(z_{\text{Init}}, \Psi_0) = (2, 2.9)$ . Shown along with them for comparison (broken lines) are the flat SCDM and (Union1-best-fit,  $\Omega_\Lambda = 0.713$ ) Concordance  $\Lambda$ CDM cosmologies.

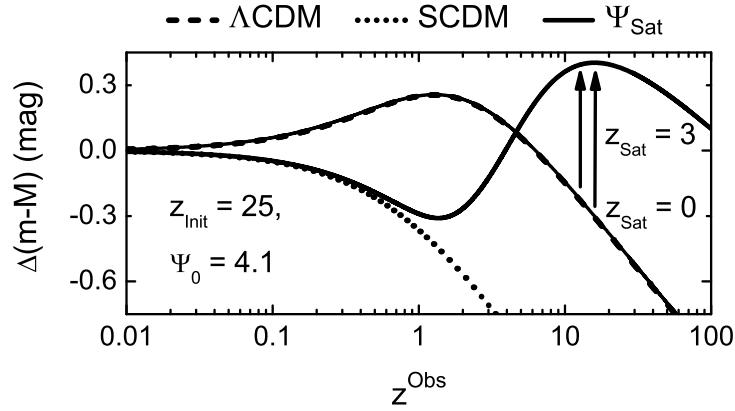


Fig. 5.— Residual Hubble diagrams for the early-saturation causal backreaction model  $\Psi_{\text{Sat}}(t)$  with  $(z_{\text{init}}, \Psi_0) = (25, 4.1)$ , where the solid line peaking at  $z^{\text{Obs}} \sim 1 - 2$  (the curve almost indistinguishable from  $\Lambda$ CDM) represents a simulated cosmology with RNL but restricted to  $z_{\text{Sat}} = 0$  (thus rendering it equivalent to  $\Psi_{\text{Sqr}}$ ); and where the solid line peaking at  $z^{\text{Obs}} \sim 10 - 20$  represents the shift to  $z_{\text{Sat}} = 3$ . Shown along with them for comparison (broken lines) are the flat SCDM and (Union1-best-fit,  $\Omega_\Lambda = 0.713$ ) Concordance  $\Lambda$ CDM cosmologies.



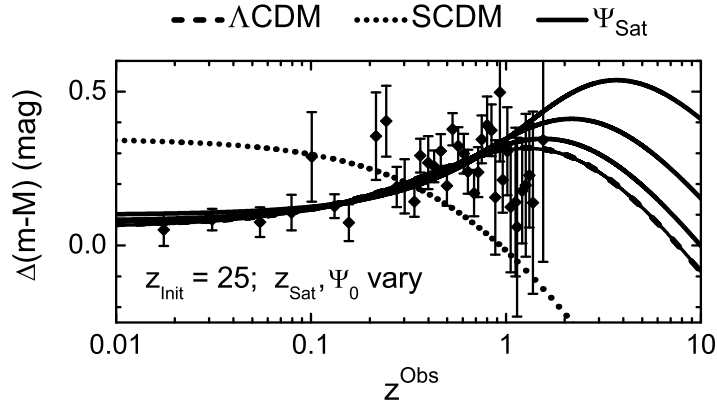


Fig. 6.— Residual Hubble diagrams for early-saturation  $\Psi_{\text{Sat}}(t)$  models with fixed  $z_{\text{Init}} = 25$  and varying  $z_{\text{Sat}}$ , with  $\Psi_0$  re-optimized for each chosen  $z_{\text{Sat}}$  value. From lowest to highest, the solid lines represent the runs with model input parameters:  $(z_{\text{Sat}}, \Psi_0) = (0, 4.1)$  (curve almost indistinguishable from  $\Lambda$ CDM);  $(z_{\text{Sat}}, \Psi_0) = (0.25, 2.6)$ ;  $(z_{\text{Sat}}, \Psi_0) = (0.5, 2.3)$ ; and  $(z_{\text{Sat}}, \Psi_0) = (1.0, 2.2)$ . Also plotted here (broken lines) are the Union1-best-fit flat SCDM and Concordance  $\Lambda$ CDM ( $\Omega_\Lambda = 0.713$ ) cosmologies. Shown along with these curves are the binned and averaged SCP Union1 SNIa data (bin size  $\Delta\text{Log}_{10}[1+z] = 0.01$ ). Each theoretical curve is displaced vertically, relative to the SNIa data, to depict its individualized  $H_0^{\text{Obs}}$ -optimization.

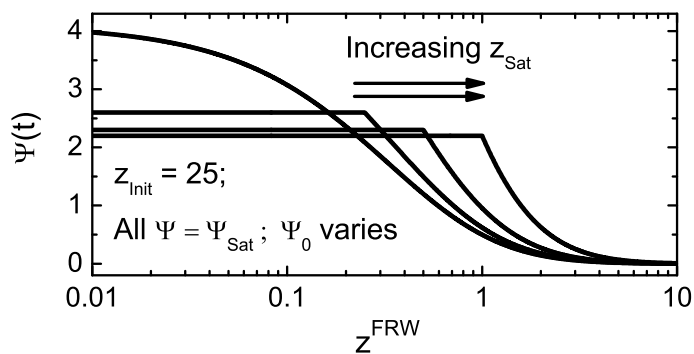


Fig. 7.— The clumping evolution functions are compared for several different early-saturation models, all with  $z_{\text{init}} = 25$ , plotted versus  $z^{\text{FRW}} \equiv [(t_0^{\text{FRW}}/t^{\text{FRW}})^{2/3} - 1]$ . In order of the positions of the functions’ ‘corners’ from left to right (increasing  $z_{\text{Sat}}$ ), the lines depict  $\Psi_{\text{Sat}}$  functions with the parameters:  $(z_{\text{Sat}}, \Psi_0) = (0, 4.1)$ ;  $(z_{\text{Sat}}, \Psi_0) = (0.25, 2.6)$ ;  $(z_{\text{Sat}}, \Psi_0) = (0.5, 2.3)$ ; and  $(z_{\text{Sat}}, \Psi_0) = (1.0, 2.2)$ .

Table 1: Supernova Fit Quality and New-Concordance Success for Optimized RNL Runs

$z_{\text{Init}}$	$\Psi_{0,\text{Opt}}$ <sup>a</sup>	$\chi_{\text{Fit}}^2$ <sup>b</sup>	Avg. % Dev. <sup>c</sup>
$\Psi_{\text{MD}}$ <i>Clumping Model Runs</i>			
1	2.8	313.0	7.5
<b>1.5</b>	<b>2.8</b>	<b>314.7</b>	<b>4.0</b>
<b>2</b>	<b>2.9</b>	<b>315.1</b>	<b>5.8</b>
3	3.1	315.5	14.1
5	3.6	317.0	30.4
10	4.3	328.5	52.2
15	4.1	339.5	51.5
20	4.1	345.8	52.6
25	4.1	349.5	53.1
$\Psi_{\text{Lin}}$ <i>Clumping Model Runs</i>			
1	3.2	311.0	7.8
1.5	3.1	312.8	5.6
<b>2</b>	<b>3.2</b>	<b>313.6</b>	<b>2.9</b>
<b>3</b>	<b>3.3</b>	<b>314.0</b>	<b>4.8</b>
5	3.6	314.3	11.9
10	4.0	314.7	21.4
15	4.3	314.9	26.7
20	4.5	315.0	30.1
25	4.7	315.1	33.0
$\Psi_{\text{Sqr}}$ <i>Clumping Model Runs</i>			
1	4.4	311.5	15.6
1.5	4.0	310.4	12.0
2	3.9	310.5	10.0
3	3.9	311.0	7.6
5	4.0	311.4	5.4
10	4.1	311.7	3.4
15	4.1	311.8	2.9
20	4.1	311.8	2.6
<b>25</b>	<b>4.1</b>	<b>311.8</b>	<b>2.5</b>

<sup>a</sup>Each  $\Psi_{0,\text{Opt}}$  chosen to minimize  $\chi_{\text{Fit}}^2$  for a given  $z_{\text{Init}}$  and  $\Psi(t)$  function.

<sup>b</sup> $\chi_{\text{Fit}}^2$  computed versus the SCP Union1 SNIa data set.

<sup>c</sup>Average Percent Deviation from the ‘‘Cosmic Concordance’’, defined (as described in the text) via cosmological parameters obtained from the Union1-best-fit  $\Lambda$ CDM model ( $\Omega_{\Lambda} = 0.713 = 1 - \Omega_{\text{M}}$ ,  $\chi_{\text{Fit}}^2 = 311.9$ ).

Table 2: Output Cosmological Parameters from our ‘Best’ Runs with Recursive Nonlinearities

$z_{\text{Init}}$	$\Psi_0$	$\chi_{\text{Fit}}^2$ <sup>a</sup>	$P_{\text{Fit}}$ <sup>b</sup>	$I_0$ <sup>c</sup>	$z^{\text{Obs}}$ <sup>d</sup>	$H_0^{\text{Obs}}$ <sup>e</sup>	$H_0^{\text{FRW}}$ <sup>f</sup>	$t_0^{\text{Obs}}$ <sup>g</sup>	$\Omega_{\text{M}}^{\text{FRW}}$ <sup>h</sup>	$w_0^{\text{Obs}}$	$j_0^{\text{Obs}}$	$l_{\text{A}}^{\text{Obs}}$
$\Psi_{\text{MD}}$ <i>Clumping Model Runs</i>												
1.5	2.8	314.7	0.324	0.53	1.16	69.54	41.96	13.95	0.948	-0.639	0.59	297.8
2	2.9	315.1	0.319	0.62	1.17	69.58	38.62	14.44	1.162	-0.639	0.51	288.7
$\Psi_{\text{Lin}}$ <i>Clumping Model Runs</i>												
2	3.2	313.6	0.340	0.53	1.16	69.75	42.10	13.88	0.946	-0.675	0.89	297.3
3	3.3	314.0	0.334	0.62	1.16	69.68	38.72	14.30	1.159	-0.667	0.83	287.2
$\Psi_{\text{Sqr}}$ <i>Clumping Model Run</i>												
25	4.1	311.8	0.367	0.53	1.14	70.07	42.32	13.64	0.943	-0.751	1.73	294.5
<i>Comparison Values from Best-Fit<sup>i</sup> flat <math>\Lambda</math>CDM Model (<math>\Omega_{\Lambda} = 0.713 = 1 - \Omega_{\text{M}}</math>)</i>												
...	...	311.9	0.380	...	1.0	69.96	69.96	13.64	0.287	-0.713	1.0	285.4
<i>Comparison Values from Best-Fit<sup>j</sup> flat SCDM Model (<math>\Omega_{\Lambda} = 0, \Omega_{\text{M}} = 1</math>)</i>												
...	...	608.2	3.4E-22	...	1.0	61.35	61.35	10.62	1.0	0.0	1.0	287.3

<sup>a</sup> $\chi_{\text{Fit}}^2$  computed versus the SCP Union1 SNIa data set.

<sup>b</sup>Each likelihood probability  $P_{\text{Fit}}$  is derived from the corresponding  $\chi_{\text{Fit}}^2$  using the  $\chi_{N_{\text{DoF}}}^2$  distribution with  $N_{\text{DoF}}$  degrees of freedom, where  $N_{\text{DoF}} = 304$  for our  $\Psi_{\text{MD}}$ ,  $\Psi_{\text{Lin}}$ , and  $\Psi_{\text{Sqr}}$  clumping models,  $N_{\text{DoF}} = 305$  for the flat  $\Lambda$ CDM model, and  $N_{\text{DoF}} = 306$  for flat SCDM.

<sup>c</sup>The integrated (Newtonian) gravitational perturbation potential at  $t_0$ , as modified by RNL, computed via Equations 15-19.

<sup>d</sup>Each  $z^{\text{Obs}}$  quoted here corresponds to  $z^{\text{FRW}} \equiv 1$ .

<sup>e</sup>The  $H_0^{\text{Obs}}$  value (given here in  $\text{km s}^{-1}\text{Mpc}^{-1}$ ) for each run is found by minimizing its  $\chi_{\text{Fit}}^2$  with respect to the SCP Union1 SNIa data set.

<sup>f</sup>Each  $H_0^{\text{FRW}}$  is computed relative to the corresponding optimized  $H_0^{\text{Obs}}$  value for that run.

<sup>g</sup>All  $t_0^{\text{Obs}}$  values are listed here in GYr, and computed assuming *no radiation* (i.e.,  $\Omega_R \equiv 0$ ).

<sup>h</sup>All  $\Omega_{\text{M}}^{\text{FRW}}$  values given here for the  $\Psi_{\text{MD}}$ ,  $\Psi_{\text{Lin}}$ , and  $\Psi_{\text{Sqr}}$  models are normalized to  $\Omega_{\text{M}}^{\text{Obs}} \equiv 0.27$ .

<sup>i</sup>“Best-Fit” for the flat  $\Lambda$ CDM Model refers here to an optimization over  $\Omega_{\Lambda}$  and  $H_0^{\text{Obs}}$ .

<sup>j</sup>“Best-Fit” for the flat SCDM Model refers here to an optimization over  $H_0^{\text{Obs}}$ .

Table 3: Output Cosmological Parameters from our RNL Runs with ‘Early Saturation’

$z_{\text{Sat}}$	$\Psi_{0,\text{Opt}}$ <sup>a</sup>	$\chi_{\text{Fit}}^2$	$P_{\text{Fit}}$ <sup>b</sup>	$I_0$	$z^{\text{Obs}}$	$H_0^{\text{Obs}}$	$H_0^{\text{FRW}}$	$t_0^{\text{Obs}}$	$\Omega_{\text{M}}^{\text{FRW}}$	$w_0^{\text{Obs}}$	$j_0^{\text{Obs}}$	$l_{\text{A}}^{\text{Obs}}$
$\Psi_{\text{Sat}}$ <i>Clumping Model Runs, <math>z_{\text{Init}} = 25</math></i>												
0	4.1	311.8	0.351	0.53	1.14	70.07	42.32	13.64	0.943	-0.751	1.73	294.5
0.25	2.6	313.5	0.326	0.58	1.15	69.60	40.24	14.00	1.054	-0.620	0.15	289.7
0.5	2.3	316.6	0.284	0.68	1.15	69.40	36.32	14.65	1.338	-0.585	-0.14	279.8
1	2.2	320.2	0.238	0.80	1.14	68.77	29.54	15.75	2.086	-0.488	-0.94	259.9
<i>Comparison Values from Best-Fit flat <math>\Lambda</math>CDM Model (<math>\Omega_{\Lambda} = 0.713 = 1 - \Omega_{\text{M}}</math>)</i>												
...	...	311.9	0.380	...	1.0	69.96	69.96	13.64	0.287	-0.713	1.0	285.4

<sup>a</sup>Each  $\Psi_{0,\text{Opt}}$  is chosen to minimize  $\chi_{\text{Fit}}^2$  for a given  $z_{\text{Sat}}$ , with  $z_{\text{Init}} = 25$  and  $\Psi(t) \equiv \Psi_{\text{Sat}}(t)$ . (Optimizations are performed with respect to the SCP Union1 SNIa data set.)

<sup>b</sup>Each likelihood probability  $P_{\text{Fit}}$  is derived from the corresponding  $\chi_{\text{Fit}}^2$  using the  $\chi_{N_{\text{DoF}}}^2$  distribution with  $N_{\text{DoF}}$  degrees of freedom, where the inclusion of optimizable parameter  $z_{\text{Sat}}$  now gives  $N_{\text{DoF}} = 303$  for our  $\Psi_{\text{Sat}}$  clumping models (even for  $z_{\text{Sat}} = 0$ ), while  $N_{\text{DoF}} = 305$  is still used here for the flat  $\Lambda$ CDM model.